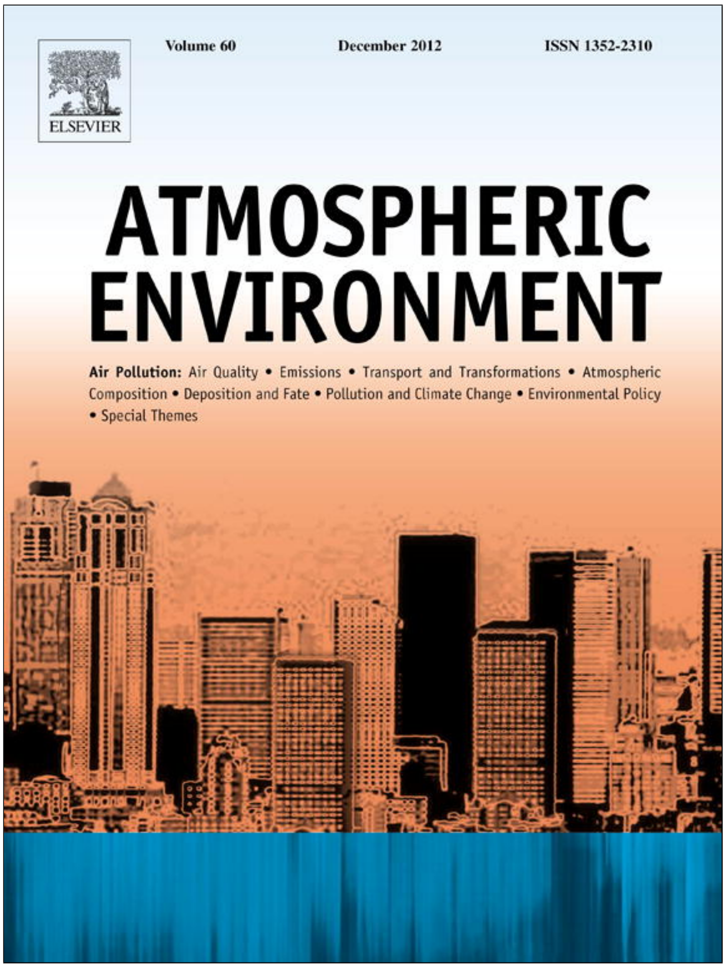
Volume 60
December 2012
ISSN 1352-2310
ELSEVIER
ATMOSPHERIC ENVIRONMENT
Air Pollution: Air Quality • Emissions • Transport and Transformations • Atmospheric Composition • Deposition and Fate • Pollution and Climate Change • Environmental Policy • Special Themes

Atmospheric Environment 60 (2012) 632–655

Contents lists available at SciVerse ScienceDirect

Atmospheric Environment

journal homepage: www.elsevier.com/locate/atmosenv

Review

Real-time air quality forecasting, part I: History, techniques, and current status

Yang Zhang [a,b,*], Marc Bocquet [c,d], Vivien Mallet [c,d], Christian Seigneur [d], Alexander Baklanov [e]

[a] Department of Marine, Earth, and Atmospheric Sciences, North Carolina State University, Raleigh, NC 27695, USA
[b] School of Environment, Tsinghua University, Beijing, China
[c] INRIA, Paris Rocquencourt Research Center, France
[d] CEREA (Atmospheric Environment Center), Joint Laboratory École des Ponts ParisTech and EDF R&D, Université Paris-Est, 77455 Marne-la-Vallée, France
[e] Research Department, Danish Meteorological Institute (DMI), Copenhagen, DK-2100, Denmark

HIGHLIGHTS

► A comprehensive review for real-time air quality forecasting (RT-AQF).
► Major milestones in the history of RT-AQF.
► Assessment of major RT-AQF techniques.
► A detailed review of 3-D RT-AQF models.
► Evaluation protocols and review of current forecasting skills of RT-AQF models.

ARTICLE INFO

Article history:
Received 6 February 2012
Received in revised form
7 June 2012
Accepted 8 June 2012

Keywords:
Air quality forecasting
Historic milestone
Techniques and tools
Evaluation methods

ABSTRACT

Real-time air quality forecasting (RT-AQF), a new discipline of the atmospheric sciences, represents one of the most far-reaching development and practical applications of science and engineering, poses unprecedented scientific, technical, and computational challenges, and generates significant opportunities for science dissemination and community participations. This two-part review provides a comprehensive assessment of the history, current status, major research and outreach challenges, and future directions of RT-AQF, with a focus on the application and improvement of three-dimensional (3-D) deterministic RT-AQF models. In Part I, major milestones in the history of RT-AQF are reviewed. The fundamentals of RT-AQF are introduced. Various RT-AQF techniques with varying degrees of sophistication and skills are described comparatively. Among all techniques, 3-D RT-AQF models with online-coupled meteorology–chemistry and their transitions from mesoscale to unified model systems across scales represent a significant advancement and would greatly enhance understanding of the underlying complex interplay of meteorology, emission, and chemistry from global to urban scales in the real atmosphere. Current major 3-D global and regional RT-AQF models in the world are reviewed in terms of model systems, component models, application scales, model inputs, forecast products, horizontal grid resolutions, and model treatments of chemistry and aerosol processes. An important trend of such models is their coupling with an urban model or a computational fluid dynamic model for urban/local scale applications at 1 km or less and with an exposure model to provide real-time public health assessment and exposure predictions. Evaluation protocols are described along with examinations of current forecasting skills and areas with large biases of major RT-AQF models.

1. Introduction

1.1. Importance and type of applications of air quality forecasting

Air quality refers to the chemical state of the atmosphere at a given time and place. Like weather, air quality affects everyone. Air pollutants include gaseous and particulate species that may lead to non-carcinogenic and/or carcinogenic adverse health effects. Numerous studies (e.g., Greenbaum et al., 2001; WHO,

* Corresponding author. Department of Marine, Earth, and Atmospheric Sciences, Campus Box 8208, NCSU, Raleigh, NC 27695, USA.
E-mail address: yang_zhang@ncsu.edu (Y. Zhang).

1352-2310/$ – see front matter
http://dx.doi.org/10.1016/j.atmosenv.2012.06.031

2004; Georgopoulos et al., 2009; Phalen and Phalen, 2011; http://www.epa.gov/apti/course422/ap7a.html) show that acute (short-term) exposure to high levels of these species may pose serious temporary health concerns such as eye irritation, difficulty breathing, pulmonary and cardio-vascular health effects and premature death. Chronic (long-term) exposure may lead to health concerns such as cancer, premature death, and damage to the body's immune, neurological, reproductive, and respiratory systems. People with pre-existing heart and lung diseases and diabetics, the elderly, and children (so-called sensitive groups) are at an even greater risk for air pollution-related health effects. In addition, these pollutants and their derivatives can cause many adverse effects on the environment including visibility impairment, acid deposition, global climate change, water quality deterioration, and plant and eco-environmental system damages (e.g., ESA, 2004; Seinfeld and Pandis, 2006; Krupa et al., 2006).

To protect human health and the environment, the World Health Organization (WHO) has issued guidelines and several countries and states have issued regulations (e.g., WHO, 2010). The U.S. Environmental Protection Agency (EPA) has set National Ambient Air Quality Standards (NAAQSs) for six air pollutants to protect human health (U.S. EPA, 1996; Seinfeld and Pandis, 2006). These pollutants are sulfur dioxide (SO_2), nitrogen dioxide (NO_2), carbon monoxide (CO), ozone (O_3), lead (Pb), and particulate matter with aerodynamic diameters less than or equal to 2.5 μm ($PM_{2.5}$) and 10 μm (PM_{10}). In Europe, the European Union (EU) issues directives, which subsequently become air quality standards or goals in 27 member states (EU, 2008). The pollutants regulated by the EU include the six pollutants regulated in the U.S. and benzene (C_6H_6), a volatile organic compound (VOC) with known carcinogenic health effects. Despite significant progress in understanding emissions and fates of these pollutants as well as in reducing their ambient levels in urban areas in the past half century, air pollution is estimated to kill 3 million people a year worldwide (http://www.world-science.net/othernews/070814_ disease.htm). In particular, PM pollution has been directly linked to excess deaths in many countries in the world (e.g., Schwartz, 1991; Dockery et al., 1993; Kunzli et al., 2000; Matanoski and Tao, 2002; Millman et al., 2008; Jayachandran, 2009; Zhang et al., 2010).

To protect citizens from unhealthy air, many countries have real-time air quality forecasting (RT-AQF) programs in place to forecast the concentrations of pollutants of special health concerns such as O_3, NO_2, $PM_{2.5}$, and PM_{10} (e.g., Manins, 1999; U.S. EPA, 1999; Pudykiewicz and Koziol, 2001). Such information has been used to issue early air quality alerts that allow government and people to take precautionary measures such as temporarily shutting off major emission sources and car pooling or taking public transportation to reduce air pollution and avoid or limit their exposures to unhealthy levels of air pollution (Wayland et al., 2002). It has been used to schedule and plan numerous field campaigns to effectively track pollutant plume transport and sample pollutant concentrations and maximize the usage of expensive instrumented platforms such as airplanes and other limited measurement resources (e.g., Lee et al., 1997; Flatøy et al., 2000). Accurate RT-AQF can therefore offer tremendous societal and economic benefits by enabling advanced planning for individuals, organizations, and communities in order to reduce pollutant emissions and their adverse health impacts.

Driven by crucial regulations, societal and economic needs, scientific advancements, and increasing availability of high performance computing capacity, RT-AQF has evolved from weather forecasting and developed into a new discipline that integrates science and technology from several disciplines including meteorology, atmospheric chemistry/air quality, mathematics, physics, environmental statistics, and computer sciences/engineering. In light of a significant progress in the past two decades and the unprecedented challenges of RT-AQF, this work intends to offer a comprehensive review of its history, current status, fundamentals, technical approaches, evaluation protocols, and improvement techniques. The objectives of this review are to summarize past achievements of RT-AQF, identify major areas of future improvement and resource investments, recommend research priorities, and provide future prospects to guide the further development of this new, exciting yet very challenging discipline for the decades to come. In the remaining Section 1, the history and current status are reviewed and the fundamentals of RT-AQF are introduced. Various RT-AQF techniques are described comparatively along with their strengths and limitations in Section 2. Major 3-D global and regional RT-AQF models are reviewed in Section 3. Evaluation protocols and current RT-AQF skills are described in Section 4.

1.2. History and current status

A sequence of severe, localized pollution episodes were reported during the 1930s-1960s. These include the Meuse Valley, Belgium, coal and coke burning smog event with 63 excess deaths and 6000 illnesses in December 1930 (Haldane, 1931); the Donora, Pennsylvania, U.S., zinc smelter smog event with 20 excess deaths and 7000 illnesses in October 1948 (Battan, 1966); and the London, U.K., coal and chemical combustion smog events with excess deaths of 4000 in December 1952, 1000 in January 1956, 300–800 in 1957, and 340–700 in 1962 (Brimblecombe, 1987). These air pollution episodes and disasters led to the passage of a number of early air pollution regulations and laws such as the Air Pollution Control Act of 1955, the Clean Air Act (CAA) of 1963, and the CAA Amendments of 1970 and 1977 in the U.S. as well as the CAA of 1956 and 1968 in Great Britain.

Table 1 summarizes the major milestones in the history of RT-AQF. In October 1954, heavy smog occurred in Los Angeles, which triggered the shutdown of schools and industry for the first time in the U.S. The Los Angeles County Air Pollution Control District (LACAPCD), the first regional air pollution control agency in the U.S., adopted a three-stage smog alert system for O_3 and three other pollutants in June 1955 to prevent the possibility of an air pollution catastrophe. In the 1960s, the U.S. Weather Bureau (USWB) (i.e., the predecessor of the National Weather Service (NWS)) provided the first forecasts of air stagnation or pollution potential by using numerical weather prediction (NWP) models to forecast conditions conducive to poor air quality (e.g., Niemeyer, 1960). These forecasts were conducted strictly from a meteorological perspective without considering the emissions and chemistry of air pollutants. In 1965, the U.S. Environmental Science Services Administration (ESSA) (the predecessor of the National Oceanic and Atmospheric Administration (NOAA)) was created. The weather officials from 25 nations met in London for the First International Clean Air Congress in 1966. In 1970, ESSA became NOAA and the USWB became NWS. The major findings of relationships between meteorological factors and air pollution potential led to the creation of the National Air Pollution Potential Forecast Program (Gross, 1970). On December 2, 1970, the U.S. EPA was created by President Nixon. In 1979, the NWS developed a global data assimilation system and its nested grid model became operational.

Starting in the 1970s, various RT-AQF techniques and tools were developed to forecast air pollution in urban areas. These techniques were largely based on empirical approaches and statistical models trained or fitted to historical air quality and meteorological data (e.g., McCollister and Wilson, 1975; Wolff and Lioy, 1978; Aron, 1980). Their level of sophistication increased considerably to overcome some of these limitations and address non-linearity of

Table 1
Selected milestones of real-time air quality forecasting (RT-AQF).

Time	Milestone
October, 1954	Heavy smog shutdown schools and industry in LA for the first time in the U.S.
June, 1955	A three-stage smog alert system was established in LA.
1960s	USWB provided the first forecasts of air stagnation or pollution potential.
1966	The First International Clean Air Congress.
1970	AFR 161-22, Environmental Pollution Control, required air-pollution potential forecasts and warnings; the national air pollution potential forecast program was established in the U.S.
1970s–1980s	Development and application of RT-AQF based on empirical approaches and statistical models.
Early 1970s to1980s	Development and application of the first-generation AQMs on urban/regional scales.
Late 1970s	The development and application of the first-generation AQMs on a global scale.
1980s–early 1990s	The development and application of the second-generation AQMs on all scales.
1990s	Application of 3-D air quality models for short-term forecasting of O_3 in several countries.
1994–1995	The first application of an operational AQF model by the University of Cambridge, U.K. to support the planning of two field experiments for stratosphere.
Mid 1990s–2000s	The development and application of the third-generation AQMs on all scales
1997	The U.S. EPA revised the AQI and established the AIRNow program to provide real-time air quality measured and forecasted data to the public; the first application of an operational AQF model by the Norwegian Institute for Air Research to support a field campaign in troposphere.
1999	The Meteorological Service of Canada (MSC) initiated an AQF program for eastern Canada; the U.S. EPA developed guideline for developing O_3 forecasting program.
Early 2000s	The U.S. Weather Research Program recommended the development and application of operational mesoscale air quality forecasts; the high-resolution advanced Weather Research and Forecasting model (WRF) was developed to serve as the backbone of the U.S. public weather forecasts and research. WRF v1.0 was released for beta test in 2001. The first official released version was v2.0 in 2004. A decision to incorporate chemistry into WRF was made at a workshop on Modeling Chemistry in Cloud and Mesoscale Models held at NCAR on March 6–8 2000.
Early 2000s-present	The development and application of the 4th-generation air quality models on all scales.
2001	MSC launched the national air quality forecast in May 2001; the first reported ensemble O_3 forecasting; the first application of chemical data assimilation for AQFs since their first applications to CTMs in mid. 1990s
2002	Under the provision of the Energy Policy Act of 2002 of USA, Congress mandated NOAA to develop nationwide RT-AQF capability for O_3. NOAA's pilot study of predicting O_3 for the New England region in 2002 using three numerical AQF model systems; the first version of WRF/Chem was released. WRF/Chem represents the first community online-coupled meteorology–chemistry model.
2003	The first RT-AQF workshop in the U.S. organized by USWRP held during April 29-May 3 in Houston, Texas; NOAA and EPA formally collaborate to develop a national RT-AQF model.
2004	The second New England Forecasting Program to forecast O_3 and $PM_{2.5}$ in the northeastern U.S. during which six numerical AQF models were deployed for RT-AQF; the U.S. EPA/NOAA's NAQFC was deployed in the summer of 2004. CFD was coupled with the 3-D AQF models for AQF over industrial plants and urban areas at horizontal grid resolutions of 1–10 m.
2005	European FUMAPEX UAQIFS with improved urban meteorology, air quality and population exposure models, were developed and launched for operational urban AQF in 6 EU cities.
2006-present	Ensemble forecast based on sole sequential aggregation; the development of the ensemble forecast of Analyses (EFA) approach to combine ensembles and data assimilation.
2007	The first large scale inverse modeling with 4D-Var data assimilation to combine emission rate and chemical state optimization in a complex 3-D AQF model (i.e., the University of Cologne mesoscale EURAD model).

the photochemical system during the 1990s (e.g., Ryan, 1995; Ryan et al., 2000). The development of 3-D numerical air quality models (AQMs) on urban, regional, and global scales since the 1970s and their applications for short- and long-term RT-AQF since the mid 1990s led to a significant frog leap. With significant advances in computational technologies and computer architectures, RT-AQF systems have shifted from postprocessing of forecast meteorology and statistical methods to the use of sophisticated 3-D AQMs that account for meteorology, emissions, chemistry, and removal processes.

3-D AQMs have evolved over four generations since the 1970s, with roughly one generation per decade, reflecting the advancements in scientific understanding and numerical and computational technologies. Review of some AQMs can be found in the literature (e.g., Seigneur, 1994, 2001; Peters et al., 1995; Russell and Dennis, 2000; Zhang, 2008). CTMs or AQMs have traditionally been used to retrospectively simulate historical poor air quality scenarios in support of regulation and planning, due primarily to computational constraints and a lack of real-time chemical measurements. Given their relative maturity in sciences and the advancement in computational technology, some of the 2nd, 3rd, and 4th generations AQMs have been deployed for RT-AQF since the mid to late 1990s. These efforts were first begun in Germany in 1994 (e.g., Rufeger et al., 1997), Japan in 1996 (e.g., Ohara et al., 1997), Australia in 1997 (e.g., Manins et al., 2002), and Canada in 1998 (e.g., Pudykiewicz and Koziol, 2001) and then expanded in the U.S. (McHenry et al., 2004; Otte et al., 2005), other countries in Europe (e.g., Brandt et al., 2001; Jakobs et al., 2002), China (Han et al., 2002; Wang et al., 2009), and other regions in Japan (Uno et al., 2003). In addition to applications to short-term forecasts of air pollution for the public, 3-D AQMs have also been applied for chemical forecasting during field campaigns. Lee et al. (1997) and Flatøy et al. (2000) represent the first RT-AQF to support the planning of field experiments for the troposphere and stratosphere, respectively. Following the two studies, a number of RT-AQFs have been applied before and during field campaigns (e.g., Kang et al., 2005; McKeen et al., 2005, 2007, 2009).

Another frog leap in the history of RT-AQF is the development of real-time data repositories such as the Aerometric Information Retrieval Now (AIRNow) network (www.airnow.gov). In 1997, the U.S. EPA developed AIRNow to provide an effective platform for communicating real-time air quality conditions and forecasts to the public via the internet and other medias. Differing from the traditional data submission, quality-control, and calibration that usually take 3–6 months after their collection, AIRNow receives real-time O_3 and PM pollution data from more than 115 U.S. and Canadian agencies as well RT-AQFs from about 400 U.S. cities and represents a centralized, nationwide, governmental repository for real-time data. AIRNow has been expanded to include real-time data from other countries such as China. Similar programs exist in the EU within the Global Monitoring for Environment and Security (GMES) Programme and the European Commission Seventh Framework Programme. Such efforts are also coordinated by several European Cooperation in Science and Technology (COST) Actions and EU networks. The air quality agency of the Paris region in France, AIRPARIF, makes real-time data available on its website. A near-real-time observation database, ***Bas**e de données en **te**mps **r**éel* (BASTER) gathers all hourly measurements made by the local air quality networks every 3 h in France, Germany, Italy, Finland, Austria, and the U.K (Rouïl et al., 2009). The U.S. EPA established the Pollutant Standard Index (PSI) (also known as the Air Pollution Index (API)) in 1978, which was replaced by the Air Quality Index (AQI) to include a simple color scheme in 1997 to link air quality concentrations and associated health effects to a simple color-coded index that can be easily and consistently reported to the public (U.S. EPA, 2000, 2009). Similar AQI/API exist in more than 37 countries in the world (e.g., Australia, Canada, Mexico, Denmark, France, U.K., Germany, China, India, Japan, Brazil, Chile).

In the mid-late 1990s, many countries recognized an increasing need to implement a centralized, national air quality forecasting system. The Minister for the Environment in Australia funded the Air Pollution in Major Cities Program and developed their RT-AQF model in 1998. The Meteorological Service of Canada (MSC) initiated an RT-AQF program for eastern Canada in 1999, which was extended to cover all of subarctic Canada in 2001 (Pudykiewicz et al., 2003). In 1999, the U.S. EPA developed a guideline for O_3 forecasting (U.S. EPA, 1999), which was extended to add $PM_{2.5}$ in 2003 (U.S. EPA, 2003). Under the provision of the Energy Policy Act of 2002 of the U.S., the U.S. Congress mandated NOAA to develop a nationwide RT-AQF capability for O_3. Since then, NOAA and EPA collaboratively developed a national RT-AQF model and provided O_3 forecast guidance to state and local forecasters (Stockwell et al., 2002; Wayland et al., 2002; Dabberdt et al., 2004). They conducted the first pilot study of predicting O_3 for the New England region in 2002 using three numerical RT-AQF models (Kang et al., 2005). The first workshop on RT-AQF in the U.S. was organized by the USWRP and held in 2003 in Houston, Texas, during which 50 scientists recommended research areas and priorities for RT-AQF that help guide the further development of the nationwide RT-AQF research program (Dabberdt et al., 2006). In 2004, NOAA sponsored the second New England Forecasting Program to forecast both O_3 and $PM_{2.5}$ in the northeastern U.S. during which 5 RT-AQF models were used for ensemble modeling (McKeen et al., 2005, 2007). The real-time National Air Quality Forecast Capability (NRT-AQFC) that consists of Eta-CMAQ, jointly-developed by U.S. NOAA and EPA, was deployed for RT-AQF in the summer of 2004; it represents the first operational forecast implementation of CMAQ (Otte et al., 2005). Region-wide efforts by universities and research organizations are prevalent in the U.S. and many countries in the world (e.g., Chen et al., 2008; Hogrefe et al., 2007; Cai et al., 2008).

Learning from initial RT-AQF applications, more sophisticated techniques such as 4-dimensional variational method (4D-Var), Kalman-filtering, and ensemble methods have been used in conjunction with 3-D RT-AQF models to improve RT-AQF results. Elbern and Schmidt (2001) conducted one of the first applications of chemical data assimilation (CDA) for RT-AQF using 4D-Var to assimilate O_3 and NO_2 observations during August 1997 over central Europe and showed a significant improvement in O_3 forecasts. The first reported ensemble O_3 forecasting was conducted with a three-member CHIMERE ensemble using three global NWPs over Europe (Vautard et al., 2001a). As one of the early real-time ensemble RT-AQFs, McKeen et al. (2005, 2007) applied several RT-AQF models to forecast O_3 and $PM_{2.5}$, respectively, during the 2004 NEAQS/ICARTT study and found that multimodel ensemble forecasting outperformed individual forecasting. The same set of RT-AQF models was applied to forecast O_3 and $PM_{2.5}$ during the TexAQS II/GoMACCS, with the ensemble forecasting performing better than most individual members (McKeen et al., 2009), which represents the first $PM_{2.5}$ ensemble, bias-corrected, and Kalman filter-corrected forecasting. Doraiswamy et al. (2009) conducted ensemble forecast of O_3 and $PM_{2.5}$ over the state of New York using CMAQ with WRF and MM5 and found that the ensemble forecasts often, but not always, perform better than individual member forecasts and the weighting or bias correction approaches may improve performance. Mallet (2010) coupled an ensemble forecasting of O_3 with CDA to overcome the limitations of pure ensemble forecasting and showed a 28% reduction in the root mean square error (RMSE). Hybrid approaches using both statistical and 3-D models have also been applied to improve the accuracy of the RT-AQF (e.g., Eben et al., 2005; Guillas et al., 2008; Kang et al., 2008; Rouïl et al., 2009). There are increasing numbers of RT-AQF applications of CTMs coupled with Computational Fluid Dynamical (CFD) models over industrial plants and urban areas at horizontal grid resolutions of 1–10 m (e.g., San José et al., 2006, 2009). These applications predict chemical concentrations in the urban canopy taking into account the complex building structure.

1.3. Fundamentals of real-time air quality forecasting

1.3.1. Major characteristics of RT-AQF

Fig. 1 shows a diagram of an RT-AQF model system from global to urban scales based on typical configurations available from current RT-AQF models. At each scale, a meteorological model and an air quality model are needed; they may be coupled online or offline. While an offline meteorological model (e.g., MM5, Grell et al., 1995 or WRF, Michalakes et al., 2001) provides meteorological forecasts separately from a regional RT-AQF model (e.g., CMAQ, Byun and Schere (2006)), an online-coupled meteorology and chemistry model (e.g., WRF/Chem, Grell et al., 2005) generates both meteorological and chemical forecasts within the same time step. At a global scale, the GCM and the global CTM (GCTM) (e.g., ECHAM5, Roeckner et al., 2006; MOCAGE, Rouïl et al., 2009), are initiated with climatological or reanalysis or observational data. The GCM produces the meteorological fields needed by the GCTM. An emission model is required to project real-time emissions based on energy/fuel consumption data at all scales. An emission processor converts projected emissions into model-ready gridded emission files. Forecasted meteorological information is needed for meteorology-dependent emissions (e.g., biogenic emissions, sea-salt and erodible dust emissions, VOC evaporation). The regional scale RT-AQF systems (e.g., CHIMERE, Rouïl et al., 2009; EURAD, Elbern et al., 2010) use meteorological initial and boundary conditions (ICONs and BCONs) from a GCM and chemical BCONs from a GCTM. Chemical ICONs from either a GCTM or observations are needed to initiate the first day's forecasting, those for subsequent days will then use previous day's forecast. The forecasting product will be post-processed and evaluated using real-time (or near real-time) observations. Products such as species concentrations and AQIs will be submitted to the medias, web sites, and subscribers. Some RT-AQF systems employ bias correction techniques to correct large, systematic biases for next-day's forecast based on previous day's forecast and observations (e.g., McKeen et al., 2005, 2007; Kang et al., 2008). The initial RT-AQFs for current day issued on a previous day may be updated in the morning based on updated meteorological forecasting to improve the accuracy of the forecasting products. Some RT-AQF systems include an extended subsystem for urban scale air quality and/or human exposure and environmental health forecasting (e.g., Tilmes et al., 2002; Baklanov et al., 2007; San José et al., 2009). The urban RT-AQF requires urban

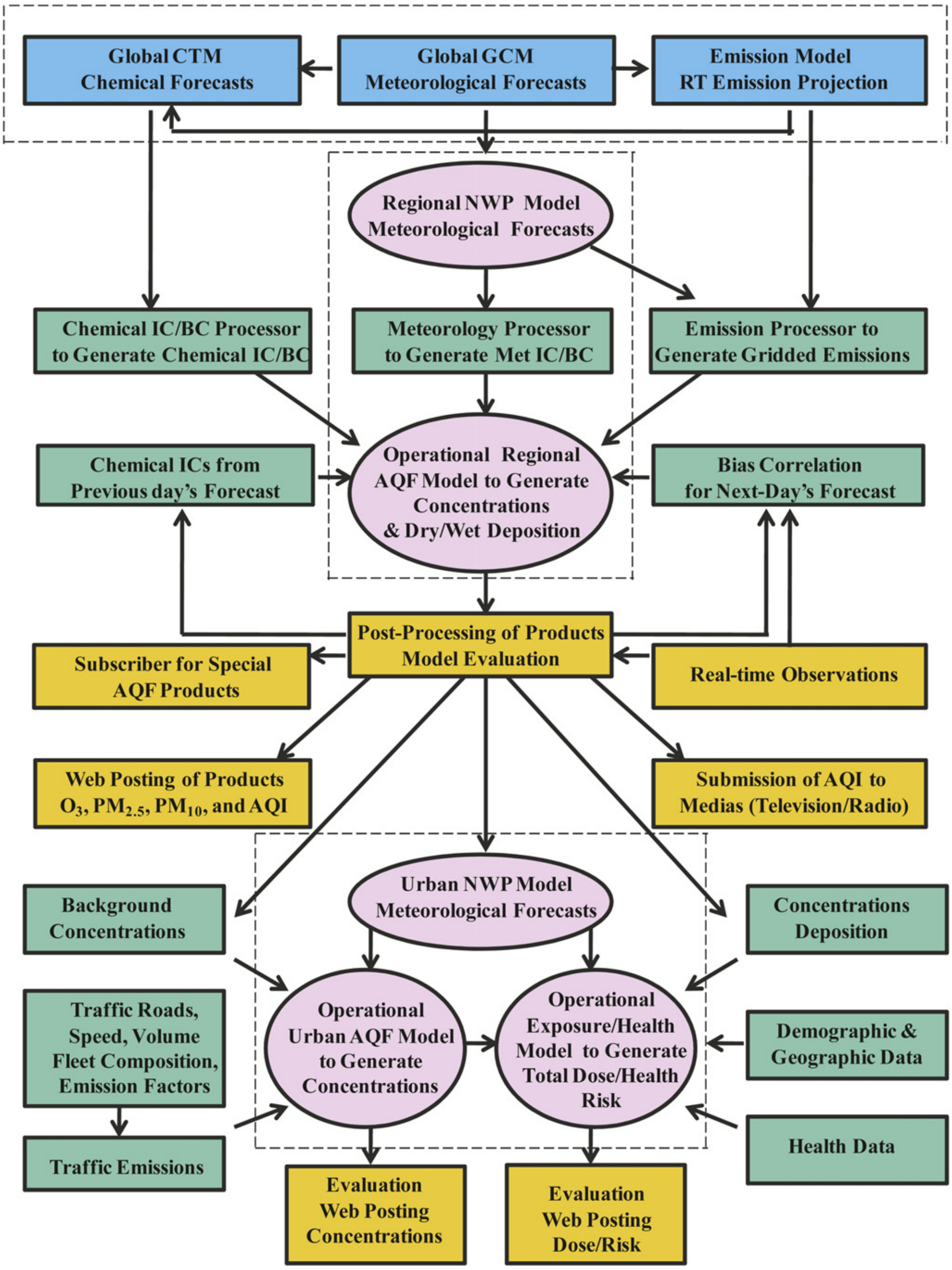

Fig. 1. An automated RT-AQF system from global to urban scales. The three model systems at global, regional, and urban scales are shown as offline-coupled meteorology–chemistry models. They can be online-coupled systems.

meteorological forecasts, background concentrations forecasted from the regional RT-AQF model, and traffic emissions that are calculated using detailed traffic information. The output includes the spatial and temporal distributions of forecasted concentrations. The neighborhood scale human exposure or environmental health forecasting requires urban meteorological forecasts, forecasted concentrations and deposition from a regional RT-AQF model, demographic and geographic data (e.g., total number of population and age distribution, location and time-activity of people), and health data (e.g., mortality, morbidity, hospital admissions) (Baklanov et al., 2007 and references therein). The output includes the spatial and temporal distributions of forecasted total dose and relative risks of adverse health outcome. The entire data retrieval, model simulation, and product processing is automated on a day-to-day basis to ensure completion of forecasts in time.

While RT-AQF is built upon weather forecasting and traditional air quality modeling, it differs from them in many aspects. RT-AQF shares the same requirements for time and optimization of model treatments as NWP but requires simulations of additional physico-chemical processes affecting fates of air pollutants; it is thus more difficult than weather forecast (Stockwell et al., 2002). While the weather forecasting is typically available for 3–10 days, RT-AQF is typically available for 1–3 days at present (e.g., STEM-2K3, Carmichael et al., 2003; WRF/Chem, McKeen et al., 2005, 2007; MOCAGE, Rouïl et al., 2009; CHIMERE, Rouïl et al., 2009), due to a much greater computational demand in terms of CPU time and disk storage required.

Compared with traditional air quality modeling for research-grade and regulatory applications, RT-AQF has its unique technical challenges and time requirements, and involves a number of real-time operational issues that did not exist before. Backcasting is driven by regulatory guidance and compliance aiming at reproducing historic pollution episodes with a high accuracy, RT-AQF is driven by societal pressures to minimize the human, environmental and economic impacts of air pollution aiming at producing warnings of high pollutant concentrations that will likely pose immediate health threats to the population. This difference leads to differences in many aspects of backcasting and RT-AQF. For example, backcasting often uses the best available model treatments to reproduce the species concentrations from a historic pollution episode; RT-AQF typically uses simplified, optimized options for dynamics, chemistry, and physics treatments that are fast enough yet reasonably accurate to meet time requirements for operational forecasting.RT-AQF often applies special techniques (e.g., bias correction, Kang et al., 2008), to achieve accuracy and computational efficiency in a very short turnaround time, which are often not needed for backcasting. While backcasting generally has no specific time window requirements, RT-AQF requires a fast short-term prediction on a day-by-day basis. This time pressure dictates the implementation of a fully automated system to download and preprocess real-time (or near real-time) datasets for RT-AQF model set up and simulations and the use of a fast set of model options for an efficient deployment of RT-AQF. For product evaluation, while RT-AQF products can be evaluated using evaluation protocols for traditional AQMs, it is more meaningful to use categorical evaluation with threshold statistics (e.g., probability of detection, false alarm ratio) (e.g., McHenry et al., 2004; McKeen et al., 2005, 2007, 2009; Kang et al., 2008), because the primary value of RT-AQFs is their guidance for issuing health advisories and alerts of an air pollution episode and the categorical indices determine the likelihood of such an episode. The end users for RT-AQF products include researchers, forecasters, regulators, decision makers in health, environmental, meteorological, and military agencies, polluters (e.g., industrialists, manufacturers, residential woodburners, car users), the public, the media (e.g., newspapers and other printed medias, television, radio, phone, pager, and internet), and the commercial sector (e.g., health insurance industry) (Dabberdt et al., 2006), which involve much larger communities than those of backcasting. RT-AQF requires a specific information technology infrastructure that is not always needed for backcasting (e.g., web-based interfaces, the construction of application-specific and/or client-oriented datasets, and a readily access to forecast products).

RT-AQF can be made for the short- or long-term, depending on the objective of the applications (Dabberdt et al., 2006). The short-term forecasts (1–5 days) will predict concentrations of pollutants and can be used daily to inform the general public about the potentially harmful conditions and to take preventive actions to reduce exposures and emissions. The long-term forecasts (>1-yr) will provide long-term variation trends of pollutants and their correlations with forecasted emissions and meteorology that can be used to guide the development of State Implementation Plans for the designated non-attainment regions. Such long-term forecasts for greenhouse gases can also be used for global climate change mitigation. This review focuses on short-term RT-AQF.

1.3.2. Forecasting products

The RT-AQF efforts since the 1990s have focused primarily on O_3 (e.g., Cope et al., 2004; McHenry et al., 2004; McKeen et al., 2005) and have only recently been expanded to include $PM_{2.5}$ and PM_{10} (e.g., McKeen et al., 2007, 2009; Chuang et al., 2011) Some also forecast other pollutants such as SO_2, NO_x, CO, VOCs, air toxics (e.g., benzene and 1,3-butadiene), and dust (e.g., Cope et al., 2004; Baklanov et al., 2007; Kaminski et al., 2008; Kallos et al., 2009; Elbern et al., 2010). For example, in Europe, NO_2 is included because of common exceedances of the air quality standard. Because there was no exceedances of the annual NO_2 standard, NO_2 has typically not been included in the U.S., although the recent promulgation of a 1-h average near-source NO_2 standard may soon generate some interest for NO_2 forecasting in North America. The forecast products are issued in terms of spatial maps or site-specific values of hourly concentrations and time-averaging concentrations (e.g., maximum 8-h average concentrations based on the U.S. NAAQS), as well as AQI. Eder et al. (2010) described approaches to use national RT-AQF guidance to develop local AQI forecasts. The AQI used in the U.S. is a dimensionless, six-color-coded index for reporting daily air quality to the public in a manner as easily understood as weather forecasts (U.S. EPA, 2009). It provides a simple, uniform system to relate daily forecasted levels of criteria pollutants (e.g., O_3, PM, NO_2, CO, and SO_2) to health advisories and alerts for sensitive groups and the general public and suggests actions to reduce exposure. Table A1 in the supplementary material shows the AQI for O_3 and PM that was established by the U.S. EPA (U.S. EPA, 2009; www.airnow.gov). The AQI converts a forecasted pollutant concentration to a number on a scale of 0–500. A value of 100 generally corresponds to the NAAQS established for each pollutant under the Clean Air Act. Values below 100 are considered satisfactory. Values above 100 indicates that the air is unhealthy and poses a health concern. For example, the 100–200 level may trigger preventive actions such as limiting certain activities and enforcing potential restrictions on industrial activities by state or local officials.

A European AQI, the Common Air Quality Index (CAQI) was developed to compare air quality in different European cities (Elshout and Léger, 2007). An important feature of CAQI is that it accounts for both urban background monitoring conditions at city background sites and traffic (i.e., near-source) pollution at/near traffic monitoring sites. The background index indicates the outdoor air quality in the city experienced by the average citizen. The obligatory background index comprises NO_2, PM_{10}, and O_3, with CO and SO_2 as auxiliary components. The traffic index indicates air quality in busy streets, which is generally the poorest air quality in the city. Citizens living, working, and visiting these streets as well as those in vehicles are all affected. The obligatory traffic index comprises NO_2 and PM_{10}, with CO as an auxiliary component. The two indices provide an improved assessment of current air quality over city averages, because some monitoring networks are designed to monitor areas of poor air quality and others provide an average city picture. CAQI has 5 levels of pollution, using a scale of 0–25 (very low), 25–50 (low), 50–75 (medium), 75–100 (high), and >100 (very high) and the matching colors are green, light green, yellow, red, and dark red, respectively.

2. Techniques and tools of RT-AQF and their advantages/limitations

Existing RT-AQF techniques and tools have various levels of sophistication and forecasting skills. They can be grouped into three categories: simple empirical approaches (also referred to as Criteria or simple rules of thumb), parametric or non-parametric statistical approaches, and more advanced, physically-based approaches. Some of them have been reviewed with varying levels of details in the literature (e.g., Wayland et al., 2002; U.S. EPA, 2003; Cope and Hess, 2005; Schere et al., 2006; Menut and Bessagnet, 2010;

Kukkonen et al., 2011). Table 2 summarizes major techniques for RT-AQF.

2.1. Simple empirical approaches

The persistence method is based on the assumption that today's observed pollutant level is tomorrow's forecasted value (U.S. EPA, 2003). As such, it requires yesterday's air quality data. This method is the quickest approach among all RT-AQF techniques. It works well under a stationary condition during which a consistently low or high pollution episode occurs but fails at the beginning or the end of the episode because it cannot handle abrupt change of weather, emissions, and air quality. Thus, it has a low accuracy from a long-term RT-AQF perspective and is primarily used as a reference (or baseline) by other methods (e.g., McHenry et al., 2004; McKeen et al., 2005, 2007, 2009).

Climatology is based on the hypothesis that air quality is highly dependent on weather, and air quality climatology is thus analogous to weather climatology. This method is computationally very fast. It uses historical frequency of pollutant events to guide and bound RT-AQF. It requires historical (>2–5 yrs) air pollutant data. Because of the averaging nature of the climatology, this method cannot account for abrupt changes in air quality due to changes in emissions (e.g., forest fires, sudden release of air toxics) and weather patterns that did not occur historically. The accuracy is low. It is not a stand-alone method and is mainly used to guide RT-AQFs derived from other methods (U.S. EPA, 2003).

Empiricism (or criteria or simple rules of thumb) is based on the assumption that thresholds (i.e., criteria) of forecasted meteorological variables can indicate future high pollutant concentrations (Wayland et al., 2002). When parameters that influence pollution are forecasted to reach a threshold, high pollutant concentrations are forecasted. This method requires observed and forecasted upper-air and surface meteorological and air quality data. It is moderately accurate. However, it cannot forecast exact concentrations and does not work for pollutants that depend weakly on weather (e.g., CO). This method relies on a strong correlation between forecasted pollutant (e.g., O_3) and meteorological variables (e.g., temperature), which may not always hold as warm temperatures are necessary but not sufficient for the formation of

Table 2
Major techniques and tools for RT-AQF.

	Strength	Limitation
Simple Empirical Approaches		
Persistence	Computationally fast; accurate during a static ambient conditions; simple to use and requires little expertise; low operational cost	Cannot handle abrupt change of weather, emissions and air quality; low accuracy; not a stand-alone method
Climatology	Computationally fast; helps guide and bound forecasts derived from other methods; Simple to use and requires little expertise; low operational cost	Cannot handle abrupt change of air quality; low accuracy; not a stand-alone method
Empiricism	Computationally fast; an effective screening method for high pollution events; simple to use; low operational cost	Cannot forecast exact concentrations; does not work for pollutants that depend weakly on weather; moderate accuracy
Parametric (Statistical) Models		
Classification and Regression Trees (CART)	Computationally fast; works well for a given site; automatically differentiates between days with similar pollutant concentrations; requires modest expertise; low operational cost; moderate/high accuracy	Cannot accurately predict extreme concentrations; limited use due to limited observations and large local-scale variations of concentrations
Regression Methods	Computationally fast; works well for a given site; commonly used and easy to operate; produces generally good forecasts; requires modest expertise; moderate operational cost; moderate/high accuracy	Cannot accurately predict extreme concentrations; the linear regression cannot handle non-linearity of the chemical system; limited use due to limited observations and large local-scale variations of concentrations
Artificial Neural Networks (ANNs)	Capacity to learn from data; works well for a given site; can handle nonlinear and chaotic chemical system at a site; requires modest expertise; moderate operational cost; moderate/high accuracy; computationally fast	Cannot accurately predict extreme concentrations; limited use due to limited observations and large local-scale variations of concentrations; poor generalization performance; moderate/high accuracy and operational cost
Fuzzy Logic Method (FL)	Capacity to represent inherent uncertainties of human knowledge; can handle non-linearity and chaotic chemical system; requires modest expertise; moderate/high accuracy; moderate operational cost	Limited use due to limited observations and large local-scale variations of concentrations; poor generalization performance; needs a substantial amount of observational data; the computational complexity due to large number of inappropriate rules
Kalman Filter Method	Provides response prediction and estimation, and associated uncertainties; allowing time dependence of parameters and components of the time series can be decomposed	Does not perform well for highly non-linear systems
Advanced, Physically-Based Approaches		
Deterministic (CTM) Models	Prognostic time- and spatially-resolved concentrations under both typical and atypical scenarios and in areas that are not monitored; scientific insights into pollutant formation processes, accounts for the air parcel history including transport issues; does not require a large quantity of measurement data; moderate/high accuracy	Biases due to imperfect and missing model treatments and inaccuracies and uncertainties in meteorological and emissions predictions and model inputs; Computationally expensive; a need for a high speed computer system; high-level of expertise; moderate/high operational cost
CTMs with Bias Correction Techniques	Combines merits of deterministic models and statistical models (or other techniques); high accuracy	Bias correction may be effective only for systematic biases and may hinder model improvement needs; computationally expensive and complex; a need for a high speed computer system; high-level of expertise; high operational cost
Ensemble and Probabilistic Methods	Improved forecast skills compared to a single member; can handle uncertainties in AQF; provides an estimate of likelihood of an occurrence of an event on a scale from 0 to 1	Observational errors are not always accounted for; inherent limitations associated with individual ensemble model member; accuracy sensitive to weighting factors; computationally very expensive and complex; a need for supercomputer system; high-level of expertise; very high operational cost

high O_3; furthermore, PM species respond differently to temperature changes. Despite these limitations, this method has been commonly used in many RT-AQF programs as a primary method or combined with other methods to screen initial RT-AQFs and determine whether the situation warrants a more quantitative RT-AQF using more sophisticated methods.

2.2. Parametric/non-parametric statistical approaches

Parametric or non-parametric statistical methods are based on the fact that weather and air quality variables are statistically related. It uses different functions (e.g., regression or trained neural network systems) to forecast pollutant concentrations that depend on external conditions. The commonly-used methods include classification and regression trees (CART) (e.g., Burrows et al., 1995), regression method (RM) (e.g., Cobourn and Hubbard, 1999; Cobourn, 2007), artificial neural networks (ANNs) (e.g., Prybutok et al., 2000; Pérez and Reyes, 2006), fuzzy logic (FL) method (e.g., Jorquera et al., 1998; Shad et al., 2009), and Kalman filter (KF) method and its variants (e.g., extended Kalman filters (EKF), square-root filters, ensemble Kalman filter (EnKF)) (e.g., van der Wal and Jansen, 2000; Zolghadri and Cazaurang, 2006). CART uses a decision tree and RM uses a regression equation to predict concentrations based on values of various meteorological and air quality parameters. ANNs and FL are artificial intelligence-based techniques. ANNs use simplified mathematical models of brain-like systems to enable a structure to simulate intelligent behavior in computers. FL uses a form of algebra with a range of values in terms of logical variables that can have continuous values between 0 and 1 (false or true, respectively) to represent varying degrees of truthfulness and falsehood (i.e., partially true or false). The main difference between FL and ANNs is that FL is a mathematical tool to deal with the uncertainties in human perception and reasoning, it can thus provide some insights into the model, whereas ANNs are fast computation tools with learning and adaptive capabilities. Kalman filtering is an efficient recursive computational solution for tracking in real time a time-dependent state vector with noisy evolution equation and with noisy measurements.

The statistical approaches usually require a large quantity of historical measured data under a variety of atmospheric conditions (e.g., 2–3 yrs observed O_3 or $PM_{2.5}$ concentrations). They are generally more suitable for the description of complex site-specific relations between concentrations of air pollutants and potential predictors, and often have a higher accuracy, as compared to deterministic models. KF provides not only the response predictions but also their associated uncertainties through the calculation of their variances and covariances. Some methods (e.g., ANNs and FL) can handle non-linearity, whereas some cannot (e.g., KF). They have several common drawbacks. First, they are usually confined to the area and conditions present during the measurements and cannot be generalized to other regions with different chemical and meteorological conditions. Second, they cannot predict concentrations during periods of unusual emissions and/or meteorological conditions that deviate significantly from the historical record (Stockwell et al., 2002). Third, they cannot capture the contribution of distant weather-dependent sources and circumstances favorable for the formation of secondary pollutants because of the use of an average relationship between local concentrations and local atmospheric conditions. Fourth, the forecast accuracy typically depends on the skill of commonly-used meteorological predictors, which usually neglect (e.g., morning inversion, regional pollutant transport) or use simplified parameterizations (e.g., turbulence, convection, and precipitation) for some meteorological processes that are important to the evolution of air pollutants (Ryan, 1995). Fifth, the nature of statistical modeling does not enable better understanding of chemical and physical processes. These statistical models provide neither the direct linkages between precursor emissions and resultant pollution nor the interrelationships among multiple pollutants (i.e., the interactions among pollutants that may potentially exacerbate one pollution problem while another problem is being alleviated). Explicit treatments for such linkages and interactions in RT-AQF models are essential to the enhancement of understanding of the physical-chemical system, the improvement of short- and long-term RT-AQF skill, and the development of integrated emission control strategies for multi-pollutants.

Various statistical approaches have been applied to RT-AQF since the late 1970s. These include multiple linear regression (e.g., Wolff and Lioy, 1978; Stadlober et al., 2008; Genc et al., 2010), CART (e.g., Burrows et al., 1995), ANNs (e.g., Pérez and Reyes, 2006; Li and Hassan, 2010), FL systems (e.g., Shad et al., 2009; Alhanafy et al., 2010), nonlinear regression (NLR) (e.g., Cobourn and Hubbard, 1999), hybrid NLR (Cobourn, 2007), and KF (e.g., Chenevez and Jensen, 2001; Hoi et al., 2008). These techniques showed some RT-AQF skill. The best techniques that can handle nonlinearities and interactive relationships include CART, ANNs, FL, and NLR, which are more accurate than linear regression (e.g., Comrie, 1997; Chaloulakou et al., 2003). Some studies (e.g., Dutot et al., 2007) showed that ANNs can outperform a CTM such as CHIMERE. To overcome their limitations, ANNs may be combined with other methods (e.g., Diaz-Robles et al., 2008).

2.3. Advanced physically-based approaches

Deterministic models of air quality (also referred to as chemical transport models (CTMs) or AQMs) explicitly represent all major meteorological, physical, and chemical processes that lead to the formation and accumulation of air pollutants by solution of the conservation equations for the mass of various species and transformation relationships among chemical species and physical states (Wayland et al., 2002). The forecasting system requires gridded meteorological fields, emissions, and chemical ICONs and BCONs. Compared with statistical methods, this approach has several strengths. First, it is capable of forecasting temporally- and spatially-resolved concentrations under both typical and atypical scenarios and pollutant concentrations in areas that are not monitored. Second, it is physically-based and provides scientific understanding of pollutant processes; thus, it can address issues that cannot be handled by other forecasting methods such as long-range transport of air pollutants, intricate interplay among meteorology, emissions, and chemistry, and changes in air quality under different meteorological and emission scenarios. Third, it offers a moderate to high accuracy, when all influential processes are accurately represented in the model. Fourth, it does not require a large quantity of measurement data. There are several drawbacks. First, it demands sound knowledge of pollution sources and processes governing their evolution in the atmosphere, making the development of such models rather difficult and costly. This crucial knowledge is often limited and/or insufficient, and in some cases, the processes may be too complex to be easily represented in a model. Approximations and simplifications are, thus, often made in CTMs. Such imperfect representations of some atmospheric processes (e.g., SOA formation) or missing treatments in current models often lead to inaccuracies and biases in forecasted concentrations. Second, the accuracy of RT-AQF depends on the accuracy of meteorological predictions, emission estimates, and other model inputs such as ICONs and BCONs. Biases in such predictions and uncertainties in model inputs can be propagated into RT-AQFs. Third, it is computationally expensive and requires a high-speed computer system with a large memory and disk storage. Despite these constraints, the use of a coupled meteorology–chemistry model for RT-AQF represents a significant advancement in routine operational RT-AQFs and would greatly enhance understanding of the underlying complex interplay of meteorology, emission, and chemistry. Since 1990s, RT-AQF systems based on CTMs have been developed rapidly and are currently in operation in many countries, including Australia, Canada, Japan, U.S., France, Denmark, Germany, Norway, U.K., Spain, Belgium, Turkey, the Netherlands, Chile, and China. Progress in CTM development and computing technologies has allowed daily RT-AQFs using simplified (e.g., Vautard et al., 2001b) or more comprehensive 3-D CTMs, such as offline-coupled (Tilmes et al., 2002; Honoré et al., 2008; Schaap et al., 2008; Chen et al., 2008; Baldasano et al., 2008; McKeen et al., 2009), and online-coupled meteorology–chemistry models (e.g., Grell et al., 2005; de Freitas et al., 2005; Baklanov et al., 2008; Flemming et al., 2009; Chuang et al., 2011). Model evaluation demonstrates that such a modeling approach has skills consistent with or better than current statistical forecasting tools (McHenry et al., 2004; Manders et al., 2009).

The use of offline-coupled meteorology and AQMs does not permit the simulation of meteorology–chemistry feedbacks such as aerosol feedbacks to radiation and photolysis, which are important and may affect the next hour's air quality and meteorological predictions (Grell et al., 2004, 2005; Zhang, 2008; Zhang et al., 2010b; Baklanov, 2010). Such systems may introduce biases in RT-AQF. For example, Otte et al. (2005) and Eder et al. (2006) reported a poor performance of their offline coupled Eta/CMAQ modeling system during cloudy periods due to neglecting aerosol feedbacks to radiation and cloud formation processes. Furthermore, atmospheric information at a time scale smaller than the output time interval of the meteorological model (e.g., 1-h) is lost in the offline-coupled model systems (Grell et al., 2004; Zhang, 2008). Online-coupled models are increasingly used for applications in which the feedbacks may be important (e.g., locations with high frequencies of clouds and large aerosol loadings), the local scale wind and circulation system change quickly, and the coupled meteorology–air quality modeling is essential for accurate model simulations (e.g., RT-AQF or simulating the impact of future climate change on air quality). Compared with offline AQMs, online models can provide more realistic treatments of the atmosphere, particularly in regions with a fast local circulation or a high aerosol loading and cloud coverage, where meteorology and radiation may be modified by the presence of chemical species through various feedback mechanisms. Therefore, an RT-AQF system that is based on an online-coupled meteorology–chemistry model can better represent the real atmosphere and thus provide more accurate RT-AQFs.

Given inherent limitations of CTMs, a number of methods have been developed to combine their use with bias correction techniques such as statistical models or data assimilation systems. Conceptually, the approach of a CTM combined with a statistical model is similar to the Model Output Statistics (MOS) (Glahn and Lowry, 1972) or a downscaling method (Wilby and Wigley, 1997) that is often used to correct biases in weather forecasting at specific sites. In this method, the linear regression model is first developed between a set of variables from the CTM and an observed variable and then used to correct forecast biases for a given site (e.g., Wilson and Valée, 2003; Honoré et al., 2008). This approach combines the strengths of CTMs and advanced observation-based techniques, thus it can have a greater accuracy than either method alone. However, the bias correction may not be effective for random errors. It may hinder the identification of problematic areas and model improvement needs. In addition, this method is computationally expensive and complex, and requires a high-level of expertise. As one of the earliest efforts exploring this method, Chenevez and Jensen (2001) applied a statistical after-treatment (i.e., an adaptive linear regression model with an optimal state estimator algorithm) of the 3-D RT-AQF to adjust the next 48-h O_3 forecasts at specific sites where real-time O_3 measurements are available. They showed that this method can give higher correlation coefficients and smaller biases/RMSEs than 3-D model raw outputs. In a post-processing step to produce reanalysis pollution maps, Honoré et al. (2008) trained MOS using past observations and then applied it to correct O_3 forecasts from the Prev'air RT-AQF system and reported large improvements in specific areas and for high O_3 levels. Konovalov et al. (2009) combined deterministic and statistical approaches for PM_{10} forecast in Europe by making statistical post-processing of forecasts from a CTM (i.e., CHIMERE) using PM_{10} monitoring data. They found that this approach significantly improved the deterministic PM_{10} forecasts with a maximum reduction of RMSE by 50%, and the maximum increase of the coefficient of determination (r^2) of more than 85%.

Several data assimilation techniques have been developed and used to improve/optimize ICONs, BCONs, emissions, and meteorology in conjunction with a CTM for RT-AQF (e.g., Elbern and Schmidt, 2001; Blond and Vautard, 2004; Chai et al., 2007; Carmichael et al., 2008; Wu et al., 2008). Blond and Vautard (2004) used a statistical interpolation method that combines O_3 predictions from CHIMERE with surface O_3 measurements for RT-AQF of O_3 for western Europe and showed that the RMSE was reduced by $\sim$1 ppb ($\sim$30% relative to the raw forecasts) for 1–2 days forecasts. Denby et al. (2008) applied two data assimilation techniques for regional PM_{10} forecasts using a 3-D RT-AQF model in Europe: statistical interpolation (SI) based on residual kriging after linear regression of the model, and EnKF. After assimilation, the root-mean square discrepancy between analyses and the observations from validation stations was reduced from 16.7 to 9.2 $\mu g\ m^{-3}$ using SI and to 13.5 $\mu g\ m^{-3}$ using EnKF, and r^2 increased from 0.21 to 0.66 using SI and to 0.41 using EnKF. Compared with a classical statistical approach (e.g., MOS), the data assimilation approach allows the use of real-time or near real-time measurements for the same day of the PM_{10} forecasts.

Another approach developed to overcome limitations of a CTM is probabilistic forecast (e.g., Wilczak et al., 2006; Delle Monache et al., 2008). There is a growing trend to shift from purely deterministic forecasts to probabilistic forecast. Given the inherent uncertainty of predictions of a CTM, probabilistic forecasts have an advantage because they provide an estimate of likelihood of an occurrence of an event (Pagowski and Grell, 2006). The simplest probabilistic forecasts are associated with a dichotomous (e.g., Yes/No) predictand. Multi-category probabilistic forecasts can provide several categories of the predictand by using a consistent set of probability values. Forecasts based on ensembles represent the third type of probabilistic forecast, in which the full distribution of probabilities, rather than categories ("maybe" versus "yes" or "no"), is approximated. Ensembles can handle uncertainties but require knowledge of model errors and uncertainties in model inputs, and different models. Also, they require a powerful computer system, a high-level of expertise, and very high operational cost. The regional RT-AQF with ten RT-AQF models over Europe within the MACC project (http://gems.ecmwf.int/d/products/raq/) represents the operational state of the art for the generation of an ensemble of forecasts.

Because of the increasing maturity of CTMs and availability of computer resources, many organizations in many countries can now afford to develop RT-AQF systems that are based on 3-D CTMs. Such physically-based RT-AQF systems represent the state of the science and will likely become prevalent forecasting approaches and tools and will be reviewed in the remaining sections.

3. Overview of major 3-D RT-AQF models on regional and global scales

3.1. Model systems, components, and application scales

A number of 3-D global and regional models have been deployed for RT-AQF. Table 3 summarizes 9 global and 36 regional RT-AQF models that are currently used in Australia, North America, South America, Europe, and Asia in terms of component models (i.e., meteorological models, air quality models, microscale models), spatial scale, and coupling between meteorology and chemistry. The full names of models and associated organizations are provided in a list of acronyms and symbols in an Appendix in the supplementary material. Among them, four global models (i.e., GEM-AQ, LMDzt-INCA, ECHAM5, and ECMWF-IFS-CTMs) and four regional models (i.e., WRF/Chem, WRF/Chem–MADRID, GEM-MACH15, and CFORS) are online-coupled models.

For global models, meteorological fields are produced by reanalysis data such as National Centers for Environmental Prediction (NCEP) or general circulation models such as GEM, ECMWF/IFS, LMDzt, ECHAM5. In unified online-coupled models such as GEM-AQ and ECHAM5, a chemistry module is incorporated into a GCM. In offline or separate online-coupled models, an AQM is driven by data from meteorological reanalysis (e.g., GOCART) or used in conjunction with a GCM (e.g., MOCAGE, MOZART-3, TM5), respectively. Among the 9 global RT-AQF models, ECMWF/IFS-CTMs that is being developed by ECMWF offers an integrated flexible, advanced global forecasting modeling tool with data assimilation of satellite observations. In ECMWF/IFS-CTMs, the IFS is coupled via a coupler software to one of the global CTMs: MOCAGE, MOZART-3, or TM5 for global forecast and assimilation of reactive chemical species. The selection of multiple CTMs and their ensemble results provides a range and an indication of the robustness of the forecasts. The coupled system can directly utilize the IFS 4D-Var algorithm to assimilate atmospheric observations (Flemming et al., 2009). Three out of 9 global models have been applied to regional domains for RT-AQF. While GEM-AQ and MOCAGE were directly downscaled to a regional domain at a finer horizontal grid resolution (Neary et al., 2007; Rouïl et al., 2009), the global-regional RT-AQF model system (GR-RT-AQF) was used to provide ICONs and BCONs to drive a regional unified online-coupled model, WRF/Chem (Takigawa et al., 2007).

For regional models, many of them use the most popular meteorological models such as MM5, WRF, and ECMWF/IFS. Many AQMs (e.g., CHIMERE and Polyphemus/Polair3D) can be driven by different meteorological models. The most commonly-used regional AQMs include CMAQ, WRF/Chem, and CHIMERE. WRF/Chem (Grell et al., 2005) and WRF/Chem–MADRID (Zhang et al., 2010a) include the most coupled meteorological, microphysical, chemical, and radiative processes and allow the simulation of aerosol direct, semi-direct, and indirect effects, thus representing the state-of-the-science online-coupled regional RT-AQF models. Since its first release in 2002, WRF/Chem has been further developed and improved by many researchers in the community (e.g., Fast et al., 2006; Zhang et al., 2010a; Shrivastava et al., 2010) and increasingly applied to many regions of the world (e.g., Tie et al., 2009; Fast et al., 2009; Misenis and Zhang, 2010; Zhang et al., 2010a,b, 2012; Li et al., 2011). Compared to WRF/Chem, WRF/Chem–MADRID includes two additional gas-phase mechanisms (i.e., the 2005 version of carbon bond gas-phase mechanism (CB05) and the 1999 Statewide Air Pollution Research Center gas-phase mechanism (SAPRC-99)), one aerosol module (i.e., the model of aerosol dynamics, reaction, ionization, and dissolution (MADRID)), one aerosol activation scheme (i.e., Fountoukis and Nenes, 2005), and several nucleation algorithms (e.g., Sihto et al., 2006; Merikanto et al., 2007; Yu, 2010). CB05 and SAPRC-99 are coupled with MADRID and two existing aerosol modules (i.e., the Modal Aerosol Dynamics Model for Europe/the Secondary Organic Aerosol Model (MADE/SORGAM) and Model for Simulating Aerosol Interactions and Chemistry (MOSAIC)) as well as the CMU aqueous-phase chemistry in WRF/Chem–MADRID (Zhang et al., 2010a, c, 2012). WRF/Chem–MADRID has been applied retrospectively over the continental U.S. and its sub-regions (e.g., Zhang et al., 2010a, 2012), and Europe (Zhang et al., 2011) and also for RT-AQF at a horizontal resolution of 12-km over the southeastern U.S. since summer 2009 (Chuang et al., 2011). Similar to the global ECMWF-IFS-CTMs, the French national air quality forecasting and monitoring system, Prev'air, consists of three models: CHIMERE, MOCAGE, and Polyphemus/Polair3D (http://www.Prev'air.org/; Rouïl et al., 2009), which allows ensemble RT-AQFs. Since spring 2003, Prev'air has been in operational forecasting. Case studies of RT-AQFs with WRF/Chem–MADRID in the eastern U.S. and Polyphemus in Europe are given in Section 7. Several RT-AQF systems are being used by regional air quality agencies (e.g., the Associations agréées de surveillance de la qualité de l'air, AASQAs) in France (e.g., AIRPARIF for the Paris region); those regional RT-AQF systems typically use CHIMERE.

Among 36 regional models, five are suitable for urban/local scale applications at a spatial resolution of 1 km or less. These models include THOR, the OPerational version of the Atmospheric Numerical pollution model for urban and regional Areas (OPANA), and four Urban Air Quality Information and Forecasting Systems (UAQIFS) models (i.e., UAQIFS – Norway, UAQIFS-Finland, UAQIFS-Italy2, and UAQIFS-Denmark). THOR includes the background urban model (BUM), the Operational Street Pollution Model (OSPM), and the Danish Rimpuff and Eulerian Accidental release Model (DREAM). OPANA includes the microscale air quality modeling system (MICROSYS) to forecast air concentrations for urban areas with street level details at a 5–10 m spatial resolution and up to 200–300 m in height over the maximum building heights in one 1-km grid cell that is nested in a regional simulation domain (San José et al., 2006, 2009). The UAQIFS models were developed as part of the Integrated Systems for Forecasting Urban Meteorology, Air Pollution, and Population Exposure – UAQIFS (FUMAPEX-UAQIFS) project sponsored by the EU (http://fumapex.dmi.dk; Baklanov, 2006). They include six separate UAQIFS that are further developed and applied in six cities in Europe. While these UAQIFS use advanced meteorological models such as HIRLAM and RAMS, the level of sophistication in AQMs varies from the simplest dispersion model with no or very simple chemistry, to the most complex 3-D AQMs such as FARM and CAMx. Their common feature lies in that they integrate the latest developments in urban meteorology, air quality, and population exposure modeling via an offline coupling approach to enhance the model's forecasting capability in urban areas. The enhanced modeling capabilities include one or more areas in urban RT-AQF, urban management and planning, public health assessment and exposure prediction, and urban emergency preparedness. One example application of an UAQIFS is given in Section 7.3.

3.2. Model input, output, and horizontal grid resolution

Table A2 summarizes model inputs and Table 4 summarizes forecast products and horizontal grid resolutions that are used in these models. For global models, anthropogenic emissions are mostly based on well known global emission inventories (e.g., the Global Emissions Inventory Activity (GEIA) and the Emission Database for Global Atmospheric Research (EDGAR)), and in some cases based on emission inventories developed in international collaborative projects (e.g., GEMS- or Megacities: Emissions, urban,

Table 3
Component Models, Spatial Scale, and Coupling of Meteorology and Chemistry in Major RT-AQF Model Systems.[a]

Country/Organization	Model System	Meteorological Model (MetM)	Air Quality Model (AQM)	Microscale Models	Scale	MetM -AQM Coupling	References
Global Models							
US/NASA	GOCART	GEOS DAS	GOCART	None	Global	Offline	Chin et al. (2003); http://acdbext.gsfc.nasa.gov/People/Chin/gocartinfo.html
Canada/York Univ.	GEM-AQ	GEM	AQ	None	Global/Regional	Unified Online	Neary et al. (2007) and Kaminski et al. (2008); http://ecoforecast.eu/index.php?id=2
France/LMD	LMDzt-INCA	ECMWF/IFS; LMDzt v4.0 with nudged with NCEP	INCA v3	None	Global	Separate Online	Hauglustaine et al. (2004) and Folberth et al. (2006); http://wwwlsceinca.cea.fr/welcome_real_time.html
France/MFCNRM	MOCAGE	ARPEGE (global) ALADIN (regional)	MOCAGE	None	Global /Regional	Offline	Rouïl et al. (2009); www.prevair.org
US/NCAR, Germany/MPIC	MATCH-NCAR	NCEP/NCAR	MATCH-NCAR	None	Global	Offline	Rasch et al. (1997) and Lawrence et al. (2003); http://www.mpchmainz.mpg.de/~lawrence/forecasts.html
Germany/MPIM	ECHAM5	ECHAM5	ECHAM5	None	Global	Unified Online	Roeckner et al. (2006) and Zhang et al. (2010); http://www.mpimet.mpg.de/en/science/models/echam.html
Norway NIAR/FLEXPART	FLEXPART	ECMWF NCEP	FLEXPART	None	Global	Offline	Forster et al. (2004) and Stohl et al. (2005); http://transport.nilu.no/flexpart
UK/ECMWF	ECMWF-IFS-CTMs	IFS	MOZART-3, TM5 or MOCAGE	None	Global	Separate online	Flemming et al. (2009) and Mangold et al. (2011); http://gems.ecmwf.int/d/products/grg/realtime/
Japan-FRCGC	GR-AQF	CCSR/NIES/FRCGC atmospheric GCM (global) WRF (regional)	CHASER (global) WRF/Chem (regional)	None	Global/Regional	Offline for global/regional Unified online for regional	Takigawa et al. (2007)
Regional Models							
Australia/CSIRO	AAQFS	LAPS	CSIRO's CTM	None	Regional	Offline	Manins (2002) and Cope et al. (2004); www.epa.vic.gov.au/Air/AAQFS
U.S./BAMS	MAQSIP-RT CMAQ	BAMS-MM5, WRF	MAQSIP CMAQ	None	Regional	Offline	McHenry et al. (2004) and McKeen et al. (2009); www.baronams.com/projects/SECMEP/index.html
U.S./WSU	AIRPACT3	MM5	CALGRID, CMAQ	None	Regional	Offline	Vaughan et al. (2004) and Chen et al. (2008); www.lar.wsu.edu/airpact-3
U.S./SUNY-Albany	AQFMS	SKIRON/Eta; WRF (NMM and ARW)	CAMx, CMAQ	None	Regional	Offline	Hogrefe et al. (2007), Cai et al. (2008) and Doraiswamy et al. (2009); asrc.albany.edu/research/aqf/
U.S./UI	STEM-2K3	MM5, WRF	STEM	None	Regional	Offline	Carmichael et al. (2003); nas.cgrer.uiowa.edu/
U.S./NOAA, EPA	NAQFC	Eta, WRF (NMM)	CMAQ	None	Regional	Offline	Otte et al. (2005), Yu et al. (2007, 2008), Lee et al. (2008) and Eder et al. (2010); www.weather.gov/aq/;airnow.gov/
U.S./NOAA	WRF/Chem	WRF (ARW)	WRF/Chem	None	Regional	Unified Online	McKeen et al. (2005, 2007); ruc.noaa.gov/wrf/WG11_RT/
U.S./NCSU	WRF/Chem-MADRID	WRF (ARW)	WRF/Chem	None	Regional	Unified Online	Zhang et al. (2010a) and Chuang et al. (2011); www.meas.ncsu.edu/aqforecasting/Real_Time.html
Canada/Environ. Canada	GEM-AURAMS	Regional GEM	AURAMS	None	Regional	Offline	McKeen et al. (2005, 2007, 2009); www.mscsmc.ec.gc.ca/research/icartt/aurams_e.html
Canada/Environ. Canada	GEM-CHRONOS	Regional GEM	CHRONOS	None	Regional	Offline	Pudykiewicz and Koziol (2001) and McKeen et al. (2005, 2007, 2009); www.msc-smc.ec.gc.ca/aq_smog/chronos_e.cfm
Canada/Environ. Canada	GEM-MACH15	GEM	chemistry from AURAMS	None	Regional	Unified Online	Talbot (2007)
France/AIRPARIF[b]	ESMERALDA	MM5	CHIMERE	None	Regional	Offline	Vautard et al. (2001a,b); http://www.esmeralda-web.fr
France/INERIS	CHIMERE	MM5, WRF, ECWMF/IFS	CHIMERE	None	Regional	Offline	Vautard et al. (2001a) and Rouïl et al. (2009); www.prevair.org

France/CEREA	POLYPHEMUS	ECMWF, MM5, WRF	Polair3D	None	Regional	Offline	Mallet and Sportisse, 2006; Mallet et al., 2007; Debry et al., 2007; Sartelet et al., 2007; cerea.enpc.fr/polyphemus/
Denmark/DMU-ATMI	THOR	The US NCEP, Eta	DEOM	BUM OSPM DREAM	Regional	Offline	Brandt et al. (2001) and Tilmes et al. (2002); luft.dmu.dk/AtmosphericEnvironment/Thor/intro_uk.html; thor.dmu.dk
Denmark/DMI	DACFOS	HIRLAM	MOON, CAMx, Enviro- HIRLAM	M2UE	Regional	Offline/online	Chenevez and Jensen (2001), Baklanov et al. (2011) and references therein
FUMAPEX UAQIFS[c]	1. UAQIFS-Norway 2. UAQIFS-Finland 3. UAQIFS-Spain 4. UAQIFS-Italy1 5. UAQIFS-Italy2 6. UAQIFS-Denmark	1. HIRLAM 2. HIRLAM 3. RAMS 4. RAMS 5. LAMI 6. HIRLAM	1. AirQUIS (dispersion) 2. CAR-FMI (dispersion) 3. CAMx (O_3 only) 4. FARM 5. NINFA-OPPIO/ADAM 6. DERMA-ARGOS	Some include population exposure models, some include urban dispersion/statistical models	Regional /local	Offline	Baklanov (2006) and Baklanov et al. (2007)
Germany/FRIUUK	EURAD	MM5	EURAD-IM	None	Regional	Offline	Elbern et al. (2010); www.eurad.uni-koeln.de
Norway/MET-NO	EMEP-Unified	ECMWF/IFS	Unified EMEP-CWF	None	Regional	Offline	Valdebenito and Benedictow (2010); www.emep.int
Sweden/SMHI	MATCH	ECMWF/IFS HIRLAM	MATCH	None	Regional	Offline	Robertson (2010); http://www.smhi.se/en/Research/Researchdepartments/ Air-quality/
Netherlands/TNO	LOTOS-EUROS	Archived analyses or ECMWF	LOTOS-EUROS	None	Regional	Offline	Schaap et al. (2008) and Manders et al. (2009); http://www.lotoseuros. nl/
Finland/FMI	SILAM v.4.5.4	ECMWF/IFS HIRLAM WRF	SILAM	None	Regional	Offline	Sofiev et al. (2006), Sofiev and Vira (2010) and Kukkonen et al. (2011); silam.fmi.fi; http://pandora.meng.auth.gr/mds/showlong.php?id=168#d_1 8
UK/AEA	WRF/CMAQ	WRF	CMAQ	None	Regional	offline	Fraser et al. (2010); www.airquality.co.uk/uk_forecasting/apfuk_home.php
UK/Met Office	NAME-III	ECMWF	NAME-III	None	Regional /local	Offline	www.airquality.co.uk/uk_forecasting/apfuk_home.php
Spain/TUM	OPANA v4.0	MM5	CMAQ	MICROSYS	Regional /local	Offline	San José et al. (2006, 2009); artico.lma.fi.upm.es
Spain/BSC-CNS	CALIOPE	WRF, MM5	CMAQ, CHIMERE, DREAM	None	Regional	Offline	Baldasano et al. (2008); www.bsc.es/caliope
Greece/UA	SKIRON/TAPM	SKIRON/dust	CAMx v4.31	None	Regional	Offline	Kallos et al. (2007, 2009), Mitsakou et al. (2008) and Spyrou et al. (2010); forecast.uoa.gr
Italy/CETEMPS	ForeChem	MM5	CHIMERE	None	Regional	Offline	Curci (2010); pumpkin.aquila.infn.it/forechem/
China/IAP-CAS	EMS-Beijing	MM5	NAQPMS, CMAQ, CAMx	None	Regional	Offline	Wang et al. (2009)
Japan/Kyushu University	CFORS	RAMS	Parameterized chemical tracers in RAMS	None	Regional	Unified Online	Uno et al. (2003), Carmichael et al. (2003) and Hadley et al. (2007)
Chile/Meteo Chile	POLYPHEMUS	MM5	Polair3D	None	Regional	Offline	Mallet et al. (2007) and Mallet and Sportisse (2006), cerea.enpc.fr/polyphemus/

[a] The list of acronyms is provided in Appendix.
[b] There are several air quality systems used by regional air quality agencies (Association agréées de surveillance de la qualité de l'air (AASQAs)) and only the one for the Paris region is given here as an example.
[c] FUMAPEX includes six UAQIFS model systems implemented in six cities in five countries, as labeled 1–6 under Model System, Meteorological Model (MetM), and Air Quality Model (AQM). UAQIFS-Italy1 refers to the UAQIFS applied for the city of Turin, Italy, and UAQIFS-Italy2 refers to the UAQIFS applied for the city of Bologna, Italy.

Table 4
Forecasting products and horizontal resolution of major RT-AQF model systems.

Organization Model System	AQF Products	Horizontal Grid Resolutions
Global Models		
US/NASA GOCART	24–96 h AQF of conc.of PM composition, total PM extinction, AOD due to SO_4^{2-}, dust, BC, OC, sea-salt, PM	2.5° × 2.5° or 1° × 1°
Canada/York Univ. GEM-AQ	5–10 days on global scale and 24–72 h on regional scale for CO, SO_2, NO_2, and O_3	Global: 1.5° × 1.5° or 0.9° × 0.9°; regional: a rotated variable resolution
France/LMD LMDzt-INCA	72 h RT AQF of O_3 and PM_{10}	2.5° × 3.75°
The Météo France MOCAGE	72-h forecasts of O_3, NO, NO_2, CO, SO_2, and PM_{10}	2° × 2° at a global scale and 0.5° × 0.5° & 0.1° × 0.15° at a regional scale
US/NCAR, Germany/MPIC MATCH-NCAR	24-h forecasts of O_3, NO_x, CO, OH, HNO_3, PAN, & VOCs	1° × 1°
Germany/MPIM ECHAM5	24-h forecasts of CO	2.8° × 2.8°
Norway NIAR/FLEXPART	72-h RT-AQF of CO, NO_x, and SO_2	1° × 1°
UK/ECMWF ECMWF-IFS-CTM	72-h RT-AQF of O_3 and CO, CO_2, $PM_{2.5}$ and composition, AOD	MOZART-3: 1.875° × 1.875° TM5 3° × 2°; MOCAGE 2° × 2°
Japan-FRCGC GR-AQF	15-h forecasts for O_3	Global: 2.8°; Japan: 15- and 5-km
Regional Models		
Australian CSIRO AAQFS	24–36 h AQF of 25 species (e.g., O_3, NO_2, CO, SO_2, VOCs, PM_1, $PM_{2.5}$, PM_{10}, visibility, and air toxics)	1–5 km
U.S./BAMS MAQSIP-RT & CMAQ	CO, ethylene, NO_y, O_3, $PM_{2.5}$, and $PM_{2.5}$ composition	45-, 15-, and 5- km
U.S./WSU AIRPACT3	24–64 h forecasts of O_3 and $PM_{2.5}$	12-km
U.S./SUNY-Albany AQFMS	24-h forecasts of CO, NO_x/NO_y, SO_2, VOC, HONO, HO_x, O_3, $PM_{2.5}$	36- and 12-km
U.S./UI STEM-2K3	48-h AQF of CO, ethylene, NO_y, O_3, $PM_{2.5}$, and $PM_{2.5}$ composition	60-, 12-, and 4-km
US NOAA/EPA's NAQFC	48-h AQF of CO, ethylene, NO_y, O_3, $PM_{2.5}$, and $PM_{2.5}$ composition	12-km
U.S. NOAA/ESRL WRF/Chem	48-h AQF of CO, ethylene, NO_y, O_3, $PM_{2.5}$, and $PM_{2.5}$ composition	12-, 27-, 36-km;
U.S./NCSU WRF/Chem-MADRID	48-h AQF of O_3, $PM_{2.5}$ and PM_{10}	12-km
Canada//EC GEM-AURAMS	48-h AQF of CO, ethylene, NO_y, O_3, $PM_{2.5}$, and $PM_{2.5}$ composition	42-, and 28-km
Canada//EC GEM-CHRONOS	48-h AQF of CO, ethylene, SO_2, NO_y, O_3, $PM_{2.5}$, PM_{10}, composition	21-km
Canada//EC GEM-MACH15	48-h forecasts of CO, SO_2, NO_2, O_3, $PM_{2.5}$, and PM_{10}	15-km
France/AIRPARIF[a]	72-h forecasts of O_3, NO_2, PM_{10}, $PM_{2.5}$	Urban: 3-km; regional: 9-km
France INERIS CHIMERE	72-h forecasts of O_3, NO, NO_2, CO, SO_2, $PM_{2.5}$, and PM_{10}	0.1°, 0.5°, 50-km
France/CEREA POLYPHEMUS	72-h RT-AQF of O_3, NO_2, $PM_{2.5}$, and PM_{10}	0.5°
Denmark DMU-ATMI THOR	72-h forecasts of O_3, NO_2, NO_x, CO	Local: 1-km; regional: 50-km
Denmark DACFOS	48-h forecast for GEMS and 36-h for DK of O_3, NO, NO_2, CO, SO_2, $PM_{2.5}$, and PM_{10}	0.2° for GEMS domain and 0.04° for inner domain
FUMAPEX UAQIFS	24–72-h AQF. Products vary with the AQF models, typically include SO_2, NO_x, CO, O_3, benzene, $PM_{2.5}$, PM_{10}, radiative tracer species, or a subset of them. Some forecasts human exposures to ambient air and radioactive pollutants	Outer grid is 12–16 km, inner/single grid is at 1–10 km, most with 2–3 levels of nesting
Germany/FRIUUK EURAD	72-h AQF of O_3, NO, NO_2, CO, C_6H_6, SO_2, $PM_{2.5}$, PM_{10}	125-, 15-, and 5- km,
Norway/MET-NO EMEP-Unified	72-h AQF of O_3, NO, NO_2, CO, SO_2, Rn-222, $PM_{2.5}$, PM_{10}	0.25°
Sweden/SMHI MATCH	72-h forecasts of O_3, NO, NO_2, CO, SO_2, $PM_{2.5}$, PM_{10}	0.5°
Netherlands/TNO LOTOS-EUROS	72-h RT-AQF of O_3, NO_2, SO_2, CO, $PM_{2.5}$, PM_{10}	0.25° (lon) × 0.125° (lat) or 0.5° × 0.25°
Finland/FMI SILAM v.4.5.4	54 to 72-h forecasts of O_3, NO, NO_2, CO, SO_2, $PM_{2.5}$, PM_{10}, Rn; 120-h forecasts of pollen	0.2°
UK/AEA WRF/CMAQ	48-h forecasting of O_3, CO, SO_2, NO_2, PM_{10} and $PM_{2.5}$	50-, 10-km
UK/Met Office NAME-III	72-h forecasts of PM tracer	50-, 8-km
Spain/TUM OPANA v4.0	72-h forecasts of O_3, NH_3, NO_2, CO, SO_2, $PM_{2.5}$, PM_{10}	Local: 10-m, regional: 9-, 3-, 1-km
Spain/BSC-CNS CALIOPE	24–72-h forecasts of O_3, NO_2, CO, SO_2, and PM_{10}	12- and 4-km
Greece/UA SKIRON/TAPM	48-h forecasts of O_3, NO_2, SO_2, SO_4^{2-}, and dust	0.25 × 0.25°
Italy/CETEMPS ForeChem	72-h forecasts of O_3, NO_2, $PM_{2.5}$, PM_{10}, and dust	0.5° and 0.15°
Chinese IAP/CAS EMS-Beijing	72–96 h forecasts of O_3, NO_2, $PM_{2.5}$, PM_{10},	81-, 27, 9, and 3-km
Japan Kyushu University CFORS	8-h AQF for SO_2, CO, EC, aerosol, Al, fine mode nss-SO4, ^{222}Radon, dust, AOD	80-km
Chile/Meteo Chile POLYPHEMUS	72-h forecast for O_3	4-km

[a] There are several air quality systems used by regional air quality agencies (e.g., Association agréées de surveillance de la qualité de l'air (AASQAs)) and only the one for the Paris region is given here as an example.

regional and Global Atmospheric POLlution and climate effects) or by individual researchers (e.g., Cooke et al., 1999). Most global models include *either online or offline* biogenic emissions. *Some models treat online or offline emissions for dust, sea salt, and* dimethyl sulfide *(DMS). Only one model (*i.e., LMDzt –INCA) treats emissions of nitrous oxides (N_2O) and methane (CH_4). Chemical ICONs are based on default settings (e.g., GOCART), 6-month spin up simulations (e.g., GEM-AQ), and other global model outputs (e.g., ECHAM5). Zero chemical ICONs are used in FLEXPART and GR_RT-AQF. Several global models constrained concentrations of some species (e.g., O_3, CH_4, NO, NO_2, HNO_3, peroxynitrous acid (HNO_4), dinitrogen pentoxide (N_2O_5), NO_y) for the upper boundary at the top of the domain based on climatology or observations to overcome the limitation associated with the lack of stratospheric chemistry and stratospheric-tropospheric exchange processes. These models provide 15–96 h RT-AQF at a horizontal grid resolution with latitude and longitude of 0.9° × 0.9° to 2.5° × 3.75°, with one exception for GEM-AQ, which can forecast up to 10 days. One notable feature of GEM-AQ is its rotated variable resolution grid with a uniform high resolution window at 0.1375° (~15-km) that can be placed over any region of interest on a regional scale (e.g., North America) (Neary et al., 2007), which makes GEM-AQ a promising model for multiscale air quality modeling. The RT-AQF products from global RT-AQF systems include gaseous species (e.g., CO, SO_2, NO_x, O_3, OH, HNO_3, peroxyacytyl nitrate (PAN), and VOCs), PM species (e.g., $PM_{2.5}$, PM_{10}, PM composition), and aerosol optical/radiative properties (e.g., aerosol extinction coefficient, AOD).

Regional RT-AQF models typically use regional anthropogenic emissions generated by GEMS-TNO/MEGAPOLI-TNO and the European Monitoring and Evaluation Programme Model (EMEP) over Europe, the U.S. National Emissions Inventory and Canadian inventories over North America, and the Transport and Chemical Evolution over the Pacific (TRACE-P) and the Intercontinental Chemical Transport Experiment-Phase B (INTEX-B) emissions over Asia, as well as national and local emission inventories (e.g., Chinese *National Environment Agency* emission inventories) over individual countries. These emissions are processed into temporally-resolved gridded emissions with emission models such as the Sparse Matrix Operator Kernel *Emissions* (*SMOKE*) *Modeling* System and the High-Elective Resolution *Modelling Emissions* System (*HERMES*). The RT-AQF models used by regional air quality agencies such as AIRPARIF for the Paris region typically use more accurate emission inventories developed based on local information than the national RT-AQF systems such as Prev'air for France. Despite the needs for real-time emissions for RT-AQF, only a few RT-AQF models (e.g., MAQSIP-RT, NRT-AQFC, WRF/Chem–MADRID, GEM-CHRONOS, CHIMERE, and Polyphemus/POLAIR3D) use projected/forecasted anthropogenic emissions for RT-AQF. For example, in NRT-AQFC, the anthropogenic emissions are calculated with two approaches: a static projection approach for emissions that are projected from historical data with predetermined spatial and temporal variability (e.g., from area sources), and an "online" approach for emissions with a strong dependence on meteorology (e.g., from point, biogenic, and mobile sources). For biogenic emissions, the Biogenic *Emissions* Inventory System (BEIS) model is used in most models. Biogenic emissions are included as offline emissions in most models and as online emissions in 7 out of 36 models. Online sea-salt and dust emissions are included in some models. Inclusion of dust emissions improves substantially the model skills in terms of both discrete and categorical statistics in regions where the influence of dust emissions cannot be neglected (e.g., over southern Europe by Jiménez-Guerrero et al., 2008). Many models do not include sources of $PM_{2.5}$ from wildfires.

Chemical ICONs are default settings that are based on climatology or measurements in most models, and spin up simulations and larger scale model outputs in some models. Chemical BCONs are based on climatology or continental clean conditions for most models and larger scale outputs for some models. These models provide 24–72 h RT-AQF at horizontal grid resolutions of 1–125 km, with an exception for CFORS that provides 8-h AQF and SILAM that provides 54–72 h forecasts of Radon, O_3, NO, NO_2, CO, SO_2, $PM_{2.5}$, and PM_{10}, and 120-h forecast for pollen. The models used by regional air quality agencies such as AIRPARIF typically use a finer spatial resolution (e.g., 3–9 km) than the national system Prev'air (e.g., 50 km). All regional models except for three models (i.e., MAQSIP-RT, THOR, and NAME III) forecast both gaseous and PM species. MAQSIP-RT forecasts O_3, THOR forecasts CO, NO_x, and O_3, and NAME-III forecasts PM tracer. AOD is forecasted only by CFORS. Among 36 models, three (i.e., UAQIFS – Norway, UAQIFS-Finland, and UAQIFS-Italy2) provide forecasts of human exposures to pollutants such as NO_2, $PM_{2.5}$, and PM_{10}.

3.3. Chemistry and aerosol treatments

Table A3 summarizes the gas-phase chemistry, aerosol chemistry and dynamics, and cloud chemistry treated in these models. The gas-phase chemistry used in global RT-AQF models ranges from highly-simplified chemical mechanisms such as SO_2 and DMS oxidation by prescribed OH radical and nitrate radical (NO_3) in GOCART (Chin et al., 2003) to a detailed chemistry such as the REactive Processes Ruling the Ozone BUdget in the Stratosphere (REPROBUS) model mechanism with 118 species and 350 reactions used in MOCAGE in the ECMWF-IFS-CTMs system (Flemming et al., 2009). Two gas-phase mechanisms that are commonly used in regional AQMs are also used in two global models, i.e., the Regional Atmospheric Chemistry Mechanism (RACM) in MOCAGE and the Carbon Bond Mechanism-Version IV (CB-IV) in TM5 in ECMWF-IFS-CTMs. SO_4^{2-}, elemental carbon (EC), primary organic carbon (OC), Na^+, Cl^-, and dust are treated in GOCART, ECHAM5, MOCAGE, and ECMWF-IFS-CTMs. Other models either include prescribed SO_4^{2-} concentrations only (e.g., LMDzt-INCA) or do not simulate PM (e.g., GR-RT-AQF). None of the nine global RT-AQF models simulate NO_3^- and secondary organic aerosol (SOA). The particle size representations are based on the modal approach with 1-mode for LMDzt-INCA and 7-mode for ECHAM5, the sectional approach with 3–12 bins for some models (e.g., GOCART, GEM-AQ), and a combination of sectional (for sea-salt and dust) and bulk (for remaining PM species) approaches for ECMWF-IFS-CTMs. The detailed aerosol microphysical processes such as nucleation, coagulation, and condensation of sulfuric acid are treated only in GEM-AQ and ECHAM5. Among 9 global RT-AQF models, only 4 models include cloud chemistry.

The most popular gas-phase chemistry mechanisms used in regional RT-AQF models include CB-IV, CB05, the carbon bond mechanism – version Z (CBM-Z), SAPRC-99, the Regional Acid Deposition Model Mechanism Version 2 (RADM2), RACM, and the ADOM version 2 (ADOM-II). These mechanisms differ in several aspects such as the number of species and reactions, the level of complexity and lumping methods for organic species, and the reaction rate/stoichiometry parameters. Among them, SAPRC-99 offers the most detailed chemistry with 80 species and 214 reactions that can lead to high O_3 formation due to high radical concentrations and chemical reactivity. Some of these gas-phase mechanisms were compared and evaluated in either box or 3-D models (e.g., Gross and Stockwell, 2003; Faraji et al., 2008; Luecken et al., 2008; Kim et al., 2009, 2011a; Zhang et al., 2012). While these mechanisms give similar predictions for gaseous concentrations in rural and clean conditions, the differences in simulated O_3 and NO_y may be large under urban conditions due mainly to different representations of organic chemistry and different selection of kinetic data for inorganic chemistry. Differences in gas-phase mechanisms will lead to differences in secondary aerosol formation. Kim et al. (2011b) reported less than 1 $\mu g\ m^{-3}$ (6%) differences in monthly-mean $PM_{2.5}$ concentrations but with up to 26% differences in $PM_{2.5}$ composition from model simulations with the same aerosol module but different gas-phase mechanisms (i.e., CB05 and RACM2). Zhang et al. (2012) compared CBM-Z, CB05, and SAPRC-99 in WRF/Chem–MADRID over the continental U.S. and found that different gas-phase mechanisms led to different predictions of concentrations of O_3 (up to 5 ppb), $PM_{2.5}$ (up to 0.5 $\mu g\ m^{-3}$), secondary inorganic $PM_{2.5}$ species (up to 1.1 $\mu g\ m^{-3}$), and organic PM (up to 1.8 $\mu g\ m^{-3}$), aerosol number concentrations (up to 41%), CCN (up to 58%), and CDNC (up to 99.7%). These studies illustrated the potentially large impact of gas-phase chemical mechanisms on overall model predictions.

Twenty regional models treat aqueous-phase equilibrium and kinetic reactions and one model (i.e., STEM-2K3) only treats equilibrium partitioning of SO_2, H_2O_2, and O_3. For models with aqueous-phase chemistry, the level of details varies from a highly-simplified (e.g., one first-order oxidation of SO_2) to the most comprehensive mechanism (e.g., the Carnegie-Mellon University (CMU) aqueous-phase mechanism with 50 aqueous-phase species, 17 aqueous-phase ionic equilibria, 21 gas-phase/aqueous-phase reversible reactions, and 109 aqueous kinetic reactions) that is used in one model (i.e., WRF/Chem–MADRID). The CMU mechanism explicitly treats the oxidation of dissolved S(IV) by H_2O_2, O_3, O_2 catalyzed by Fe^{3+} and Mn^{2+}, and radical species, as well as the non-reactive uptake of HNO_3, hydrochloric acid (HCl), ammonia (NH_3), and other trace gases.

Compared with global RT-AQF models, regional RT-AQF models contain much more detailed aerosol treatments. All models except for THOR and five UAQIFS models simulate SO_4^{2-}, NO_3^-, NH_4^+, EC, OC, sodium and chloride. UAQIFS-Spain and UAQIFS-Denmark do not simulate PM. Other models only simulate some PM species. Wind-blown dust is simulated in 14 out of 36 models (e.g., ART-AQFS, STEM-2K3, WRF/Chem, CHIMERE, SKIRON/TAPM). 21 out of 36 models simulate detailed aerosol chemistry and dynamics such as thermodynamics for inorganic and organic aerosols, nucleation, condensation, and coagulation. Three models (i.e., EMEP-Unified, MATCH, and LOTOS-EUROS) only simulate thermodynamics for inorganic aerosols, and GEM-CHRONOS simulates an additional process, i.e., SOA formation using a fixed yield approach. Nine models (e.g., ART-AQFS, MAQSIP-RT, THOR) do not simulate any aerosol chemistry and dynamics.

Among the three CTMs in Prev'air, Polyphemus/Polair3D contains drivers for simple forward run (forecast), ensemble forecast, and various data assimilation methods and offers the most detailed chemistry and aerosol treatments. For example, it includes two aerosol models: a Modal Aerosol Model (MAM, Sartelet et al., 2007) and a SIze REsolved Aerosol Model (SIREAM, Debry et al., 2007). SIREAM simulates detailed aerosol chemistry and dynamic processes using state-of-the-science algorithm. SOA formation is simulated using either an improved version of the SORGAM model (Kim et al., 2011b), which is based on an absorptive partitioning theory and treats eight SOA classes (4 anthropogenic and 4 biogenic), or the AER/EPRI/Caltech (AEC) SOA model (Kim et al., 2011a), which is based on a hydrophobic/hydrophilic molecule-based gas-partitioning scheme. Currently, most SOA modules used in most RT-AQF models do not take into account the hydrophilic behavior of organic species and only a few account for SOA formation from oxidation of gaseous precursors such as isoprene and sesquiterpene.

4. Evaluation protocols and model performance of 3-D RT-AQF models

4.1. Evaluation protocols

Two types of evaluations are typically conducted to evaluate the model's forecasting skills: discrete evaluation that uses a set of statistical measures and categorical evaluation that uses a set of categorical indices. Tables 5 and 6 summarize major statistical measures and categorical indices commonly used, respectively. Statistical measures and evaluation protocol for discrete evaluation of RT-AQF are the same as those recommended by Seigneur et al. (2000), U.S. EPA (2001), and Yu et al. (2006) for traditional AQMs. The traditional statistical measures include correlation coefficient (r), mean bias (MB), mean absolute gross error (MAGE), RMSE, mean normalized bias (MNB), mean normalized gross error (MNGE), normalized mean bias (NMB), normalized mean gross error (NMGE), fractional bias (FB), and fractional gross error (FGE). Some problems may arise with some of those traditional measures. For example, overpredictions are artificially given more weight than underpredictions when MNB/MNGE and NMB/NMGE are used, because MNB and NMB can grow disproportionally for overpredictions but are bounded by -1 for underpredictions (Seigneur et al., 2000). A set of new statistical metrics was therefore developed by Yu et al. (2006) based on the concept of factors to overcome the limitations of the traditional measures. These new metrics include the mean normalized factor bias (MNFB), the mean normalized gross factor error (MNGFE), the normalized mean bias factor (NMBF), and the normalized mean error factor (NMEF). While MNFB and MNGFE are still subjected to the dominance by the extremely low observational values in the normalization, NMBF and NMEF provide the most robust statistical measures, and are therefore recommended for operational evaluation for model predictions (Yu et al., 2006). In addition, peak accuracy measures (e.g., unpaired peak accuracy (UPA), temporally-paired peak accuracy (TPPA), spatially-paired peak accuracy (SPPA), and pair peak accuracy (PPA)), index of agreement (IOA), and Brier score (BS) are often used in the discrete evaluation. UPA quantifies the difference between the magnitude of the peak observed and simulated values in the modeling domain, regardless whether this occurs at the monitoring station and time of the peak observed value. UPA tests the model's ability to reproduce the highest observed value anywhere in the region. UPA is less useful as the two peak values may not occur at the same location and time. TPPA, SPPA, and PPA provide more stringent measures. TPPA tests the model's ability to reproduce the highest observed value at the hour of the peak observed value at any location within the modeling domain. SPPA tests the model's ability to reproduce the highest observed value at the monitoring station of the peak observed value at any hour. PPA tests the model's ability to reproduce the highest observed value at the time and location of the peak observed value, which is the most stringent measure among the four peak accuracy measures. IOA provides a measure of how well the departure of the simulated values from the observed mean matches with the departure of observations from the observed mean. An IOA of 1 indicates a perfect agreement. BS measures the average squared deviation between predicted probabilities for a set of events and their outcomes, so a lower score represents a higher accuracy. It is a measure used frequently for probabilistic forecasts.

The traditional categorical indices include accuracy (A), critical success index (CSI) or threat score (TS), probability of detection (POD) (or hit rate (HRate)), bias (B), false alarm ratio (FAR), false alarm rate (FARate), Heidke skill score (HSS), Pierce skill score (PSS) (or true skill score (TSS) or Hansen and Kuipers discriminant (HKD)), skill score (SS), and economic value (EV). A indicates the percentage of forecasts that correctly predicts an exceedance or a nonexceedance. CSI indicates the percentage of the forecasted actual exceedances to all actual and forecasted exceedances. POD or HRate indicates the percentage of the forecasted actual exceedances to all actual exceedances. CSI is a more balanced score because it takes into account both missed exceedances and false alarms whereas POD does not take into account false alarms. B judges if forecasts are underpredicted (<1, also referred to as underforecasting, or "false negative") or overpredicted (>1, also referred to as overforecasting, or "false positive"). FAR measures the percentage of times an exceedance was forecast when exceedance did not occur. FARate indicates the proportion of nonexceedances that were incorrectly forecasted (i.e., the probability of false detection), it is the counterpart to the hit rate, POD, or HRate. HSS measures the fractional improvement of the forecast (i.e., the total number of correct forecasts minus the correct random forecasts) over the standard random chance forecasts (i.e., the total number of forecasts minus the correct forecasts due to chance). Like most skill scores, it is normalized by the total range of possible improvement over the standard, which means HSS can safely be compared on different datasets. PSS (or TSS or HKD) measures skills relative to an unbiased random reference forecast by taking the differences between POD and FARate. SS measures the relative accuracy with respect to a set of reference forecasts. The most convenient reference is the persistence forecast. Any valid error metrics such as RMSE and NME can be used to calculate

Table 5
Discrete statistical measures used in the model evaluation (compiled from Willmott, 1981; Zhang et al., 2006a; Yu et al., 2006; Dutot et al., 2007).

Metrics	Mathematical Expression[a]	Range
Correlation Coefficient	$r = \left\{\sum_{i=1}^{N}(M_i - \overline{M})(O_i - \overline{O})\right\} \Big/ \left\{\sum_{i=1}^{N}(M_i - \overline{M})^2 \sum_{i=1}^{N}(O_i - \overline{O})^2\right\}^{\frac{1}{2}}$	−1 to 1
Mean Bias (MB)	$\mathrm{MB} = \frac{1}{N}\sum_{i=1}^{N}(M_i - O_i) = \overline{M} - \overline{O}$	$-\infty$ to $+\infty$
Mean Absolute Gross Error (MAGE)	$\mathrm{MAGE} = \frac{1}{N}\sum_{i=1}^{N}\lvert M_i - O_i\rvert$	0 to $+\infty$
Root Mean Square Error (RMSE)	$\mathrm{RMSE} = \left[\frac{1}{N}\sum_{i=1}^{N}(M_i - O_i)^2\right]^{\frac{1}{2}}$	0 to $+\infty$
Mean Normalized Bias (MNB)	$\mathrm{MNB} = \frac{1}{N}\sum_{i=1}^{N}[(M_i - O_i)/O_i] = \frac{1}{N}\sum_{i=1}^{N}(M_i/O_i - 1)$	−1 to $+\infty$
Mean Normalized Gross Error (MNGE)	$\mathrm{MNGE} = \frac{1}{N}\sum_{i=1}^{N}[(\lvert M_i - O_i\rvert)/O_i]$	0 to $+\infty$
Normalized Mean Bias (NMB)	$\mathrm{NMB} = \sum_{i=1}^{N}(M_i - O_i) \Big/ \sum_{i=1}^{N}O_i = \frac{\overline{M}}{\overline{O}} - 1$	−1 to $+\infty$
Normalized Mean Error (NME)	$\mathrm{NME} = \sum_{i=1}^{N}\lvert M_i - O_i\rvert \Big/ \sum_{i=1}^{N}O_i = \mathrm{MAGE}/\overline{O}$	0 to $+\infty$
Fractional Bias (FB)	$\mathrm{FB} = \frac{1}{N}\sum_{i=1}^{N}\frac{M_i - O_i}{(M_i + O_i)/2}$	−2 to +2
Fractional Gross Error (FGE)	$\mathrm{FGE} = \frac{1}{N}\sum_{i=1}^{N}\frac{\lvert M_i - O_i\rvert}{(M_i + O_i)/2}$	0 to 2
Mean Normalized Factor Bias (MNFB)	$\mathrm{MNFB} = \frac{1}{N}\sum_{i=1}^{N}F_i$, where $F_i = M_i/O_i - 1.0$ for $M_i \geq O_i$, $F_i = 1.0 - O_i/M_i$ for $M_i < O_i$	$-\infty$ to $+\infty$
Mean Normalized Gross Factor Error (MNGFE)	$\mathrm{MNGFE} = \frac{1}{N}\sum_{i=1}^{N}\lvert F_i\rvert$, where $F_i = M_i/O_i - 1.0$ for $M_i \geq O_i$, $F_i = 1.0 - O_i/M_i$ for $M_i < O_i$	0 to $+\infty$
Normalized Mean Bias Factor (NMBF)	$\mathrm{NMBF} = \sum_{i=1}^{N}M_i \Big/ \sum_{i=1}^{N}O_i - 1 = \overline{M}/\overline{O} - 1$, for $\overline{M} \geq \overline{O}$ $\mathrm{NMBF} = 1 - \sum_{i=1}^{N}O_i \Big/ \sum_{i=1}^{N}M_i = (1 - \overline{O}/\overline{M})$, for $\overline{M} < \overline{O}$	$-\infty$ to $+\infty$
Normalized Mean Error Factor (NMEF)	$\mathrm{NMEF} = \sum_{i=1}^{N}\lvert M_i - O_i\rvert \Big/ \sum_{i=1}^{N}O_i = \frac{\mathrm{MAGE}}{\overline{O}}$, for $\overline{M} \geq \overline{O}$, $\mathrm{NMEF} = \sum_{i=1}^{N}\lvert M_i - O_i\rvert \Big/ \sum_{i=1}^{N}M_i = \frac{\mathrm{MAGE}}{\overline{M}}$, for $\overline{M} < \overline{O}$	0 to $+\infty$
Unpaired peak accuracy (UPA)	$\mathrm{UPA} = \frac{M_{\max,x,t} - O_{\max,\hat{x},\hat{t}}}{O_{\max,\hat{x},\hat{t}}}$	−1 to $+\infty$
Temporally-paired peak accuracy (PPA)	$\mathrm{TPPA} = \frac{M_{\max,x,\hat{t}} - O_{\max,\hat{x},\hat{t}}}{O_{\max,\hat{x},\hat{t}}}$	−1 to $+\infty$
Spatially-paired peak accuracy (SPPA)	$\mathrm{SPPA} = \frac{M_{\max,\hat{x},t} - O_{\max,\hat{x},\hat{t}}}{O_{\max,\hat{x},\hat{t}}}$	−1 to $+\infty$
Paired peak accuracy (PPA)	$\mathrm{PPA} = \frac{M_{\max,\hat{x},\hat{t}} - O_{\max,\hat{x},\hat{t}}}{O_{\max,\hat{x},\hat{t}}}$	−1 to $+\infty$
Index of Agreement (IOA)	$\mathrm{IOA} = 1 - \frac{\sum_{i=1}^{N}(M_i - O_i)^2}{\sum_{i=1}^{N}(\lvert M_i - \overline{O}\rvert + \lvert O_i - \overline{O}\rvert)^2}$	0 to 1
Brier Score (BS)	$\mathrm{BS} = \frac{1}{K}\sum_{t=1}^{K}(p_t - o_t)^2$	0 to +1

N is the number of samples (by time and/or location). $M_{\max,\hat{x},\hat{t}}$ and $O_{\max,\hat{x},\hat{t}}$ are time- and space-paired peak simulated and observed values, with the circumflex indicating that the peak value occurs at the time t and location x of the peak observed value. p_t and o_t are the probability that an event occurs according to an ensemble and the event actually occurred or not at instance t (0 if it doesn't happen and 1 if it happens), respectively. K is the number of forecasting instances.
[a] $\overline{M} = (1/N)\sum_{i=1}^{N}M_i, \overline{O} = (1/N)\sum_{i=1}^{N}O_i$, M_i and O_i are values of model predictions and observations at time or location i, respectively.

SS. For a perfect model, A, CSI, POD, HSS, PSS, and SS would be 1, FAR and FARate would be zero, and B would be unity.

The above traditional categorical metrics provide "clear cut" measures of the model's ability to predict an "exceedance" by using a fixed threshold concentration and time- and space-paired observation–forecast sets. A main limitation is that they cannot provide information regarding the spatial variations of pollutant concentrations within a region of interest. To overcome this limitation, Kang et al. (2007) developed three new categorical metrics for RT-AQF evaluation: the weighted success index (WSI), area hit

Table 6
Categorical statistical measures used in the model evaluation (compiled based on Ryan, 1995; McHenry et al., 2004; Kang et al., 2005, 2007; Pagowski and Grell, 2006).

Metrics	Mathematical Expression[a]	Range
Accuracy	$A = \frac{b+c}{a+b+c+d}$	0–1
	$CSI = \frac{b}{a+b+d}$	0–1
Critical Success Index or Threat Score (TS)	$WSI = \frac{b+\sum_1^n IP}{a+b+d}$	0–1
The Weighted Success Index (WSI)[b]	$IP = \frac{M_i - f\times O_i}{M_i - f\times T}, \quad \text{for } M_i > T > O_i \text{ and } M_i < f\times T$ $IP = \frac{O_i - f\times M_i}{O_i - f\times T}, \quad \text{for } O_i > T > M_i \text{ and } O_i < f\times M_i$ $IP = 0, \quad \text{for other conditions}$	
Probability Of Detection Or Hit Rate	$POD = H = \frac{b}{b+d}$	0–1
Area Hit Rate[c]	$aH = \frac{Ab}{Ab+Ad}$	0–1
Bias or Bias Ratio	$B = \frac{a+b}{b+d}$	0 to $+\infty$
False Alarm Ratio	$FAR = \frac{a}{a+b}$	0–1
Area False Alarm Ratio[d]	$aFAR = \frac{Aa}{Aa+Ab}$	0–1
False Alarm rate	$FARate = F = \frac{a}{a+c}$	0–1
Heidke skill score	$HSS = \frac{2(bc-ad)}{(b+d)(c+d)+(a+b)(a+c)}$	$-\infty$ to 1
Pierce skill score (or true skill score (TSS), or Hansen and Kuipers discriminant)	$PSS = POD - FARate = \frac{b}{b+d} - \frac{a}{a+c} = \frac{bc-ad}{(a+c)\times(b+d)}$	−1 to 1
Skill score[e,f]	$SS = \frac{E_m - E_{ref}}{E_{perf} - E_{ref}}$ $E_m = RMSE = \left[\frac{1}{N}\sum_{i=1}^{N}(M_i - O_i)^2\right]^{\frac{1}{2}}$ $\text{or } NME = \left[\sum_{i=1}^{N}\lvert M_i - O_i\rvert\right] \Big/ \sum_{i=1}^{N} O_i = MAGE/\overline{O}$ $E_{ref} = RMSE = \left[\frac{1}{N}\sum_{i=1}^{N}(M_i - K_i)^2\right]^{\frac{1}{2}}$ $\text{or } NME = \left[\sum_{i=1}^{N}\lvert M_i - M_j\rvert\right] \Big/ \sum_{j=1}^{N} K_i = MAGE_{ref}/\overline{K}$ $E_{perf} = 0$	0–1
Economic value (EV)	$EV = \frac{\min(r,cf) - F(1-cf)r + H\,cf(1-r) - cf}{\min(r,cf) - cf\,r}$ $r = \frac{C}{L} = \frac{a+b}{d}$ $H = \frac{b}{b+d}$ $F = \frac{a}{a+c}$ *cf* is the climatological frequency of an event.	0–1

[a] Where a, b, c, d, are the number of simulated and observed data pairs at one site at a specific time in the four regions (see Table below) that represent forecast exceedances that did not occur, forecast exceedances that did occur, forecast nonexceedances that did occur, and forecast nonexceedances that did not occur, respectively.Contingency table for threshold forecasts.

		Observed	
		Yes	No
Forecast	Yes	*b*	*a*
	No	*d*	*c*

[b] M_i and O_i are values of model prediction and observation at a location *i*, respectively. *T* is the threshold value used. *f* is an empirical factor that reflects the zone in which the most points are located on the prediction–observation scatterplots, its typical value can be 1–2.

[c] *Ab* is the number of exceedances that are both observed and forecast but the forecast is any exceedance that occurs in the designated area centered at the monitor location. *Ad* is the number of observed exceedances that are not forecast within the designated area centered at the monitor location.

[d] *Aa* is the number of forecast area exceedances that were not observed and Ab is the number of forecast exceedances that were observed.

[e] M_i, O_i, and K_i are values of model prediction, observation, and temporal or spatial persistence value at time or location *i*, respectively. Temporal persistence value is the previous day's forecast value. Spatial persistence value is the observation at the nearest location to the location *i*. $\overline{O} = (1/N)\sum_{i=1}^{N} O_i$, $\overline{K} = (1/N)\sum_{i=1}^{N} K_i$, *N* is the number of samples (by time and/or location), RMSE – Root mean square error, NME – Normalized mean error, MAGE – Mean Absolute Gross Error.

[f] E_m, E_{ref}, and E_{perf} are the errors associated with model, reference, and perfect forecast, respectively. E_m and E_{ref} can be any valid error metrics, e.g., *RMSE* and *NME*. The temporal or spatial persistence forecast is often used as a reference forecast, a perfect forecast has a zero error, i.e., $E_{perf} = 0$.

(aH), and area false-alarm ratio (aFAR). WSI is less stringent than CSI, but a more representative measure. It provides partial credit to observation–forecast pairs that fall just outside limits established by CSI but within a designated factor that is used to judge the model performance (e.g., data pairs fall into a factor of 1–2 of the observations).

An important, practical aspect of RT-AQFs is how forecasts can be used to mitigate the impact of air quality on economy and people. In the calculation of EV, one needs to know the climatological frequency (*cf*) of an event, in addition to the values of *a*, *b*, *c*, and *d* (see definitions in Table 6). Hits and false alarms incur a cost of taking a preventive action (C), while misses are associated with losses due to the lack of prevention (L). Correct rejections (c) incur no expense. EV is defined as the reduction in mean expense, relative to the reduction (both defined with respect to *cf*) that would occur if all the forecasts were correct (Pagowski and Grell, 2006). As for weather forecasting, EV provides a useful measure for the economic benefits of the existing RT-AQFs and the benefits of improving these systems to individuals, businesses, and society.

No recommended values of performance statistics were provided for acceptable forecasting skills by any individual countries. The recommended values for retrospective AQ modeling can provide some guidance for RT-AQF skill evaluation. For example, Zhang et al. (2006a) recommended the use of MNBs and NMBs $\leq$ 15%, MNGEs and NMEs $\leq$ 30% as indications of a satisfactory performance for O_3 and $PM_{2.5}$. Boylan and Russell (2006) recommended the use of mean fractional bias (MFB) and mean fractional error (MFE) for PM, with good performance indicted by MFBs $\leq \pm$30% and MFEs $\leq$ 50% for $PM_{2.5}$ and MFBs $\leq \pm$60% and MFEs $\leq$ 75% for major PM components that have concentrations $\geq$ 2.25 $\mu g\ m^{-3}$. The U.S. EPA recommended that a so-called weight of evidence approach in which a set of diverse analyses are used to judge model performance. Since no single statistical metrics can fully reflect RT-AQF skill, discrete and categorical statistics summarized in Tables 5 and 6 are recommended to provide a comprehensive evaluation of an RT-AQF system.

4.2. Observational datasets for model evaluation

Datasets for forecasting evaluation and improvement include real-time or near real-time surface measurement datasets, such as the U.S. EPA's AIRNOW, datasets obtained by aircraft, ship, ozonesondes, and lidars during special field campaigns and satellite data. Satellite observations can complement datasets from surface networks by providing derived chemical measurements. Recent work has shown the potential of using near real-time satellite and surface data to improve RT-AQF (e.g., Al-Saadi et al., 2005; Kondragunta et al., 2008; Wang et al., 2011). Over Europe, the Global and Regional Earth-System Monitoring Using Satellite and In situ Data (GEMS) and MACC projects are aimed at a near real-time data assimilation and forecast capability for aerosols, greenhouse gases, and reactive gases. The dataset can be used to monitor the composition, infer estimates of surface fluxes, and produce global, short-range, and medium-range forecasts.

4.3. Current model forecasting skills

Most evaluations of forecasted O_3 and its precursors focus on summer, and very few include winter (e.g., Manins et al., 2002; Cai et al., 2008; Doraiswamy et al., 2009). Forecasting PM is more difficult than forecasting O_3 because PM consists of multiple chemical components over a broad size spectrum. PM modeling is starting to reach sufficient maturity for transition from research to operational use. Several PM models have recently been transferred into operational models to forecast PM (Carmichael et al., 2003; McHenry et al., 2004; McKeen et al., 2005, 2007; Yu et al., 2008; Chuang et al., 2011), very few studies provide detailed evaluations of forecasted PM and its composition and precursors (e.g., McKeen et al., 2007, 2009; Yu et al., 2008; Chen et al., 2008; Manders et al., 2009). Similar to O_3 forecasts, most evaluations are conducted for summer episodes, and very few for winter episodes (e.g., Mathur et al., 2008; Konovalov et al., 2009) or a full year (e.g., Manders et al., 2009). Limited evaluation was performed for coarse particles such as mineral dust (e.g., Jiménez-Guerrero et al., 2008; Niu et al., 2008; Menut et al., 2009) that may be of major concerns for PM_{10} attainment in some regions such as Asia, southern Europe, and the western U.S. Jiménez-Guerrero et al. (2008) showed that the inclusion of a dust emission module substantially increases the accuracy of both discrete and categorical statistics in the Iberian Peninsula in Europe where the influence of the Saharan dust cannot be neglected.

Table A4 summarizes the evaluation of a number of RT-AQF systems in terms of domain and period and discrete and categorical performance statistics. While maximum 1-h O_3 average statistics are generally satisfactory, those for maximum 8-h average and hourly O_3 sometime exceed NMB of 15% and NME of 30% for some models (e.g., Eta/CMAQ, WRF-NMM/CMAQ) over the eastern or northeastern U.S. in the O_3 season during 2004–2006, indicating a relatively poor performance. The overpredictions in the low O_3 range (<50 ppb) were reported in several studies (e.g., Yu et al., 2007; Chen et al., 2008). Several factors may contribute to such overpredictions. These include a poor representation of the nocturnal PBL mixing height (Gilliam et al., 2006; Zhang et al., 2006b; Eder et al., 2006); an excessive downward transport of high level O_3 aloft and too much photolysis under high cloud conditions (Eder et al., 2006); a high O_3 production rate with the SAPRC-99 chemical mechanism (Arnold and Dennis, 2006); the model limitation in resolving titration of O_3 by NO in urban plumes (Yu et al., 2007); and the BCONs from global models (Chen et al., 2008). Chuang et al. (2011) applied WRF/Chem–MADRID for RT-AQF and found that O_3 overprediction in most regions in the southeastern U.S. is likely caused by inaccurate emissions of precursors such as biogenic VOCs, positive biases in 2-m temperature and negative biases in wind speed at 10-m. O_3 underpredictions in some regions could be due in part to the uncertainties in lateral BCONs.

For categorical evaluation, different threshold values were used for the same variables. For example, the threshold values used for maximum 1-h average O_3, maximum 8-h average O_3, and hourly O_3 are 60–125 ppb, 65–85 ppb, and 80 ppb, respectively. Some of these values are lower than the former U.S. NAAQS of 120 ppb for maximum 1-h average O_3 and the current U.S. NAAQS of 75 ppb for maximum 8-h O_3, respectively, for the reasons stated previously (e.g., Hogrefe et al., 2007; Yu et al., 2007; Chuang et al., 2011), although higher thresholds were used in some earlier applications (e.g., Kang et al., 2005). For maximum 1-h average O_3, A, CSI, POD, B, and FAR range from 15 to 99.8%, 5.2 to 21.6%, 6.9 to 89%, 0.1 to 5.3 ppb, and 0.3 to 94.1%, respectively. Prev'air gives the lowest A of 15–41%, because it underestimates O_3 daily maxima at high O_3 concentrations (Honoré et al., 2008). All RT-AQFs give low values of CSI and POD but higher values of FAR because they fail to forecast exceedance (i.e., a low value of b) but overpredict low O_3 (i.e., a high value of a). A, CSI, POD, B, and FAR for maximum 8-h average O_3 range from 76.2 to 99.8%, 0 to 53.2%, 0 to 84.8%, 0.3 to 17.0 ppb, and 13 to 99.1%, respectively. Compared with maximum 1-h O_3, the values of CSI and POD are higher and those of FAR are lower for corresponding maximum 8-h O_3. The categorical evaluation for hourly O_3 was conducted by only one model (i.e., WRF/Chem–MADRID), with A, CSI, POD, B, and FAR of 99.2%, 2.5%, 18.8%, 6.8 ppb, and 97.2%, respectively. Very few evaluations were conducted for precursors of O_3 and other gaseous species (e.g., Cai et al., 2008) and vertical profile of forecasted concentrations (e.g., Yu et al., 2007). Yu et al. (2007) reported that Eta/CMAQ reproduced O_3 vertical distributions on most of the days at low altitudes, but overpredictions occurred at altitudes > 6 km because of a combination of effects related to the specifications of meteorological lateral BCONs as well as the model's coarse vertical resolution in the upper free troposphere.

Surface PM forecasts are evaluated in terms of 24-h average $PM_{2.5}$, hourly $PM_{2.5}$, and 24-h average PM_{10}. These evaluations, however, have been very limited to date and a consistent evaluation protocol has not yet been well established (Seigneur, 2001; Zhang et al., 2006a). The forecasting skill for $PM_{2.5}$ is overall poorer than that for O_3. For 24-h average $PM_{2.5}$, MBs, RMSEs, NMBs, and NMEs range from −3.2 to 6.2 μg m^{-3}, 1.7 to 15.9 μg m^{-3}, −21 to 32%, and 37 to 81%, respectively. The NMB of −21% using Eta/CMAQ over the eastern U.S. during July 14–August 18, 2004 was reported by Yu et al. (2008), who attributed underpredictions to underestimated total carbonaceous PM at both urban and rural sites and a significant underestimation of unspecified anthropogenic PM mass (mainly consisting of primary emitted trace elements) at rural sites. On the other hand, Hogrefe et al. (2007) showed that Eta/CMAQ overpredicted $PM_{2.5}$ in the New York City due to overpredictions in organic aerosols and crustal material. Factors contributing to such overpredictions include underpredictions of nocturnal vertical mixing, inaccurate temporal allocation of primary OM emissions, and underestimate of deposition processes. Chen et al. (2008) reported the NMB of 17–32% over the Pacific Northwest during August–November 2004. The overpredictions in $PM_{2.5}$ were attributed to uncertainties in wildfire emission estimates and the modeling error in fire plume transport due to errors in MM5-predicted wind direction and wind speed. McKeen et al. (2007) evaluated RT-AQF of 6 models including WRF/Chem at two grid resolutions (12- and 36-km), CHRONOS, AURAMS, STEM-2K3, and Eta/CMAQ. They found that most models did not reproduce the observed diurnal variation at urban and suburban sites, particularly during the nighttime to early morning and the ensemble mean based on 6 models with equal weighting gave the best possible forecast in terms of statistics. Chuang et al. (2011) showed slight underpredictions of $PM_{2.5}$ in the O_3 season over the southeastern U.S. by WRF/Chem–MADRID, which were attributed to uncertainties in emissions such as those of biogenic VOCs and NH_3, overpredictions of precipitation, and uncertainties in the BCONs. Only two studies evaluated hourly $PM_{2.5}$, giving MBs, RMSEs, NMBs, and NMEs of −3.3 to −0.6 μg m^{-3}, 8.3–11.3 μg m^{-3}, −21.1 to −5.2%, and 49.8–51.4%, respectively. For 24-h average PM_{10}, MBs and RMSEs range from −29 to 13.8 μg m^{-3} and 8.3 to 47.2 μg m^{-3}, respectively. Berge et al. (2002) reported forecasted PM_{10} performance over Oslo with an MB of −20.9 μg m^{-3} and an NMB of −36.5% at Kirkeveien due to an inaccurate emissions of PM_{10} from the surface (i.e., the re-suspension of dust deposited at the roadside) on dry days and an MB of 13.8 μg m^{-3} and an NMB of 24% at Furuset due to errors in simulated grid-averaged wind fields.

Very few evaluations were conducted for PM components. McKeen et al. (2007) found that all the six RT-AQF models significantly underpredicted OM at the surface and overestimated SO_4^{2-} above 2 km. The overpredictions in SO_4^{2-} were attributed to overestimate of SO_2 by WRF/Chem and CHRONOS and the inclusion of aqueous-phase oxidation of SO_2 by AURAMS, CMAQ/ETA, and STEM-2K3. Yu et al. (2007) reported that Eta/CMAQ overpredicted SO_4^{2-} due to too much in-cloud SO_2 oxidation as a result of overestimated H_2O_2 concentrations in the model, underpredicted NH_4^+ at the rural sites and aloft due to the exclusion of some sources of NH_3 in the real-time emission inventory, underpredicted NO_3^- due to overpredictions of SO_4^{2-}, and underpredicted OC due to missing sources of primary OC in the emission inventory and missing SOA formation from the gas-phase oxidation of isoprene and sesquiterpenes and aqueous-phase oxidation of glyoxal and methylglyoxal. Chen et al. (2008) reported that AIRPACT-3 reproduced OC well but significantly overpredicted EC and significantly underpredicted SO_4^{2-}, NO_3^-, and NH_4^+, due to underestimation of emissions of primary PM species (e.g., sulfate) and precursors of secondary PM (e.g., SO_2, NH_3, and NO_x), insufficient spatial resolution, and model's inability to capture the hourly PM variations.

For categorical evaluation of PM, some studies used threshold values of 15–31.5 μg m^{-3} for 24-h average $PM_{2.5}$ and 30–50 μg m^{-3} for 24-h average PM_{10} that are lower than the NAAQSs of 24-h average $PM_{2.5}$ of 35 μg m^{-3} and 24-h average PM_{10} of 150 μg m^{-3} for the same reason as mentioned previously. For 24-h average $PM_{2.5}$, A, CSI, POD, B, and FAR range from 60.8 to 99.7%, 0 to 53.7%, 0 to 90.9%, 0.7 to 1.9 μg m^{-3}, and 25 to 100%, respectively. Those for 24-h average PM_{10} range from 16.7 to 100%, 9.1 to 100%, 15.0 to 100%, 0.5 to 0.9 μg m^{-3}, and 0 to 4.8%, respectively. Categorical evaluation of hourly $PM_{2.5}$, was conducted only with WRF/Chem–MADRID, with A, CSI, POD, B, and FAR of 72.1%, 20.5%, 29.2%, 0.7 μg m^{-3}, and 59.1%, respectively.

5. Summary of Current States of RT-AQF

Emerging as a new discipline of applied sciences that integrates several physical sciences, mathematical/statistical tools, and computer technology in the 1970s, RT-AQF represents a unique applied science affecting human's daily activities and poses unprecedented challenges intersecting many aspects of sciences and technologies. Driven by deteriorated air quality worldwide, increased societal/human demands, and rapid scientific and technological advancements, significant progress has been made in the past four decades in RT-AQF. A number of RT-AQF tools and models with varying degrees of sophistication and forecasting skills ranging from the simplest rule of thumb to the most advanced 3-D online-coupled meteorology–chemistry models have been developed. Among them, the deterministic physically-based RT-AQF models that are based on 3-D global and regional CTMs represent the state of the science, enabling scientific understanding of mechanisms for pollutant formation and development of emission control strategies. Although other approaches, in particular, parametric (statistical) models, will continue to be used, the 3-D RT-AQF models will likely become prevalent approaches and tools on all the scales. There is a growing trend to combine these 3-D models with statistical models to provide more accurate RT-AQF. Among all RT-AQF models, the coupled meteorology–chemistry model represents a significant advancement and will greatly enhance the understanding of the underlying complex interplay of meteorology, emissions, and chemistry in the real atmosphere. Important extensions of the RT-AQF models include their coupling with an urban model (e.g., traffic and/or local pollutant dispersion) or a CFD model for urban/local scale applications at a spatial resolution of 1 km or less and with an exposure model to provide real-time public health assessment and exposure predictions, and urban emergency preparedness.

3-D RT-AQF models have been used for 24–72 h RT-AQF worldwide since the mid 1990s. Despite their unique characteristics and technical requirements, 3-D RT-AQF models are based on NWP models and CTM development and application efforts in the past decades and, therefore, are subject to limitations of these models. Although no universal forecasting guidance and evaluation protocols were developed covering all countries, some guidance and protocols were recommended by governmental agencies and the scientific community. Discrete and categorical evaluations are two most commonly-used evaluations. Real-time or near real-time surface air quality measurement and satellite datasets are increasingly available for such evaluations. The evaluation efforts have been primarily focused on O_3, NO_2, and PM (both PM_{10} and $PM_{2.5}$) at surface level. The forecasting skill is typically better for O_3 than for $PM_{2.5}$. While their performance statistics averaged over a time period (e.g., monthly or daily) and the whole domain is generally good or satisfactory, current RT-AQF models have difficulties forecasting variations at finer time scales (hourly and diurnally) and individual monitoring stations. In addition, larger biases exist for forecasted NO_x, HONO, HNO_3, and OH and PM composition including SO_4^{2-}, NO_3^-, and OM, indicating possible error compensations that lead to current levels of forecast accuracy. These forecast inaccuracies have been attributed to a number of factors that are highly uncertain or lack of accurate treatments in the RT-AQF models including mesoscale meteorological processes (e.g., sea-breeze circulations) and variables (e.g., temperature, PBL height), chemical BCONs of O_3 and $PM_{2.5}$, emissions (e.g., SO_2, NO_x, NH_3, BVOCs, primary PM), physical and chemical processes (e.g., urban processes, in-cloud oxidation of SO_2, SOA formation), and model configuration (e.g., coarse grid resolution). Recent advances have been made in some of those aspects. Part II of this review will assess and discuss these advances along with advanced computational techniques that can potentially improve RT-AQF. Recommendations for research priorities and future prospects will also be provided.

Acknowledgments

This work was performed under the Fellowship Award (#704389J), Center for Education and Research/École des Ponts ParisTech, France, through a visiting professorship at the Atmospheric Environment Center (CEREA), the Joint Laboratory École des Ponts ParisTech and EDF R&D, Paris, France; the NSF Career Award (#ATM-0348819); the EPA-Science to Achieve Results (STAR) program (#R83337601), and China's National Basic Research Program (2010CB951803). Support from CEEH, MEGAPOLI and COST ES1004 is also acknowledged. Thanks are due to Ming-Tung Chuang, a former post-D researcher at NCSU, for compiling an earlier version of Table A4. Thanks are due to Yelva Roustan, Atmospheric Research Center (CEREA), France; Christian Hogrefe, the New York State Department of Environmental Conservation (*NYSDEC), NY, U.S.;* and John McHenry, Baron Advanced Meteorological Systems (*BAMS*), U.S. for providing some information regarding their air quality forecasting models.

Appendix A. Supplementary Material

Supplementary data related to this article can be found online at http://dx.doi.org/10.1016/j.atmosenv.2012.06.031.

References

Alhanafy, T.E., Zaghlool, F., El, A.S., Moustafa, D., 2010. Neuro fuzzy modeling scheme for the prediction of air pollution. J. American Sci. 6 (12), 605–616.

Al-Saadi, J., Szykman, J., Pierce, R.B., Kittaka, C., Neil, D., Chu, D.A., Remer, L., Gumley, L., Prins, E., Weinstock, L., MacDonald, C., Wayland, R., Dimmick, F., Fishman, J., 2005. Improving national air quality forecasts with satellite aerosol observations. Bull. Amer. Meteor. Soc. 86, 1249–1261.

Arnold, J.R., Dennis, R.L., 2006. Testing CMAQ chemistry sensitivities in base case and emissions control runs at SEARCH and SOS99 surface sites in the southeastern US. Atmos. Environ. 40, 5027–5040.

Aron, R.H., 1980. Forecasting high level oxidant concentrations in the Los Angeles basin. J. Air Pollut. Control Assoc. 20, 1227–1228.

Baklanov, A., Hänninen, O., Slordal, L.H., Kukkonen, J., Bjergene, N., Fay, B., Finardi, S., Hoe, S.C., Jantunen, M., Karppinen, A., Rasmussen, A., Skouloudis, A., Sokhi, R.S., Sorensen, j. H., Ødegaard, V., 2007. Integrated systems for forecasting urban meteorology, air pollution and population exposure. Atmos. Chem. Phys. 7, 855–874. www.atmos-chem-phys.net/7/855/2007/.

Baklanov, A., Korsholm, U., Mahura, A., Petersen, C., Gross, A., 2008. Enviro-HIRLAM: on-line coupled modelling of urban meteorology and air pollution. Adv. Sci. Res. 2, 41–46. www.adv-sci-res.net/2/41/2008/.

Baklanov, A., Mahura, A., Sokhi, R. (Eds.), 2011. Integrated Systems of Meso-Meteorological and Chemical Transport Models, first ed. Springer, ISBN 978-3-642-13979-6, p. 242.

Baklanov, A., 2006. Overview of the European project FUMAPEX. Atmos. Chem. Phys. 6, 2005–2015.

Baklanov, A., 2010. Chemical weather forecasting: a new concept of integrated modeling. Adv. Sci. Res. 4, 23–27.

Baldasano, J.M., Jiménez-Guerrero, P., Jorba, O., Pérez, C., López, E., Güereca, P., Martin, F., García-Vivanco, M., Palomino, I., Querol, X., Pandolfi, M., Sanz, M.J., Diéguez, J.J., 2008. CALIOPE: an operational air quality forecasting system for the Iberian Peninsula, Balearic Islands and Canary Islands – First annual evaluation and ongoing developments. Adv. Sci. Res. 2, 89–98. ISSN 1992-0628, May.

Battan, L.J., 1966. The Unclean Sky. Doubleday, Garden City, N.Y, 141 pp.

Berge, E., Walker, S.-E., Sorteberg, A., Lenkopane, M., Eastwood, S., Jablonska, H.I., . Koltzow, M.Ø., 2002. A real-time operational forecast model for meteorology and air quality during peak air pollution episodes in Oslo, Norway. Water Air Soil Poll.: Focus 2, 745–757.

Blond, N., Vautard, R., 2004. Three-dimensional ozone analysis and their use for short-term ozone forecasts. J. Geophys. Res. 109, D17303. http://dx.doi.org/10.1029/2004JD004515.

Boylan, J.W., Russell, A.G., 2006. PM and light extinction model performance metrics, goals, and criteria for three-dimensional air quality models. Atmos. Environ. 40 (26), 4946–4959. http://dx.doi.org/10.1016/j.atmosenv.2005.09.087.

Brandt, J., Christensen, J.H., Frohn, L.M., Palmgren, F., Berkowicz, R., Zlatev, Z., 2001. Operational air pollution forecasts from European to local scale. Atmos. Environ. 35 (Suppl. 1), S91–S98.

Brimblecombe, P., 1987. The Big Smoke: a History of Air Pollution in London since Medieval Time. Routledge Revivals, Methuen, London, U.K, 186 pp.

Burrows, W.R., Benjamin, M., Beauchamp, S., Lord, E.R., McCollor, D., Thomson, B., 1995. CART decision-tree statistical analysis and prediction of summer season maximum surface ozone for the Vancouver, Montreal, and Atlantic Regions of Canada. J. Appl. Meteor. Climatol. 34, 1848–1862.

Byun, D., Schere, K.L., 2006. Review of the governing equations, computational algorithms, and other components of the models-3 community multiscale air quality (CMAQ) modeling system. Appl. Mech. Rev. 59, 51–77.

Cai, C., Hogrefe, C., Katsafados, P., Kallos, G., Beauharnois, M., Schwab, J.J., Ren, X., Brune, W., Zhou, X., He, Y., Demerjian, K., 2008. Performance evaluation of an air quality forecast modeling system for a summer and winter season – Photochemical oxidants and their precursors. Atmos. Environ. 42, 8585–8599. http://dx.doi.org/10.1026/j.atmosenv.2008.08.029.

Carmichael, G.R., et al., 2003. Regional-scale chemical transport modeling in support of intensive field experiments: overview and analysis of the TRACE-P observations. J. Geophys. Res. 108 (D21), 8823. http://dx.doi.org/10.1029/2002JD003117.

Carmichael, G.R., Sandu, A., Chai, T., Daescu, D.N., Constantinescu, E.M., Tang, Y., 2008. Predicting air quality: improvements through advanced methods to integrate models and measurements. J. Comput. Phys. 227, 3540–3571.

Chai, T., Carmichael, G.R., Tang, Y., Sandu, A., Streets, D.G., 2007. Four-dimensional data assimilation experiments with international consortium for atmospheric research on transport and transformation ozone measurements. J. Geophys. Res. 112, D12S15. http://dx.doi.org/10.1029/2006JD007763.

Chaloulakou, A., Saisana, M., Spyrellis, N., 2003. Comparative assessment of neural networks and regression models for forecasting summertime ozone in Athens. Sci. Total Environ. 313, 1–13.

Chen, J., Vaughan, J., Avise, J., O'Neill, S., Lamb, B., 2008. Enhancement and evaluation of the AIRPACT ozone and $PM_{2.5}$ forecast system for the Pacific Northwest. J. Geophys. Res. 113, D14305. http://dx.doi.org/10.1029/2007JD009554.

Chenevez, J., Jensen, C.O., 2001. Operational ozone forecasts for the region of Copenhagen by the Danish Meteorological Institute. Atmos. Environ. 35, 4567–4580.

Chin, M., Ginoux, P., Lucchesi, R., Huebert, B., Weber, R., Anderson, T., Masonis, S., Blomquist, B., Bandy, A., Thornton, D., 2003. A global aerosol model forecast for the ACE-Asia field experiment. J. Geophys. Res. 108 (D23), 8654. http://dx.doi.org/10.1029/2003JD003642.

Chuang, M.-T., Zhang, Y., Kang, D.-W., 2011. Application of WRF/Chem-MADRID for real-time air quality forecasting over the southeastern United States. Atmos. Environ. 45 (34), 6241–6250.

Cobourn, W.G., Hubbard, M.C., 1999. An enhanced ozone forecasting model using air mass trajectory analysis. Atmos. Environ. 33, 4663–4674.

Cobourn, W.G., 2007. Accuracy and reliability of an automated air quality forecast system for ozone in seven Kentucky metropolitan areas. Atmos. Environ. 41, 5863–5875. http://dx.doi.org/10.1016/j.atmosenv.2007.03.024.

Comrie, A.C., 1997. Comparing neural networks and regression models for ozone forecasting. J. Air & Waste Manag. Assoc. 47, 653–663.

Cooke, W.F., Liousse, C., Cachier, H., Feichter, J., 1999. Construction of a fossil fuel emission data set for carbonaceous aerosol and implementation and radiative impact in the ECHAM4 model. J. Geophys. Res. 104, 22137–22162.

Cope, M.E., Hess, G.D., 2005. Air quality forecasting: a review and comparison of the approaches used internationally and in Australia. Clean Air and Environ. Quality 39 (1), 52–60.

Cope, M.E., Hess, G.D., Lee, S., Tory, K., Azzi, M., Carras, J., Lilley, W., Manins, P.C., Nelson, P., Ng, L., Puri, K., Wong, N., Walsh, S., .Young, M., 2004. The Australian air quality forecasting system. Part I: project description and early outcomes. J. Appl. Meteorol. 43, 649–662.

Curci, G., 2010, An air quality forecasting tool over Italy. In: Proceedings of 31st Technical Meeting on Air Pollution Modelling and its Application, Torino, Italy, September.

Dabberdt, W.F., Carroll, M.A., Baumgardner, D., Carmichael, G., Cohen, R., Dye, T., Ellis, J., Grell, G., Grimmond, S., Hannaa, S., Irwin, J., Lamb, B., Madronich, S., McQueen, J., Meagher, J., Odman, T., Pleim, J., Schmid, H.P., Westphal, D.L., 2004. Meteorological research needs for improved air quality forecasting: report of the 11th prospectus development team of the U. S. Weather Research Program. Bull. Amer. Meteor. Soc. 85, 563–586.

Dabberdt, W.F., Carroll, M.A., Appleby, W., Baumgardner, D., Carmichael, G., Davidson, P., Doran, J.C., Dye, T.S., Grimmond, S., Middeleton, P., Neff, W., Zhang, Y., 2006. USWRP workshop on air quality forecasting. Bull. Amer. Meteor. Soc. 86, 215–221.

de Freitas, E.D., Martins, L.D., Silva Dias, P.L., Fátima Andrade, M., 2005. A simple photochemical module implemented in RAMS for tropospheric ozone concentration forecast in the metropolitan area of São Paulo, Brazil: coupling and validation. Atmos. Environ. 39, 6352–6361.

Debry, É., Fahey, K., Sartelet, K., Sportisse, B., Tombette, M., 2007. Technical note: a new size REsolved Aerosol Model: SIREAM. Atmos. Chem. Phys. 7, 1537–1547.

Delle Monache, L., Wilczak, J., McKeen, S., Grell, G., Pagowski, M., Peckham, S., Stull, R., McHenry, J., McQueen, J., 2008. A Kalman filter bias correction method applied to deterministic, ensemble averaged, and probabilistic forecasts of surface ozone. Tellus, Ser. B 60, 238–249. http://dx.doi.org/10.1111/j.1600-0889.2007.00332.x.

Denby, B., Schaap, M., Segers, A., Builtjes, P., Horálek, J., 2008. Comparison of two data assimilation methods for assessing PM_{10} exceedances on the European scale. Atmos. Environ. 42, 7122–7134.

Diaz-Robles, L.A., Ortega, J.C., Fu, J.S., Reed, G.D., Chow, J.C., Watson, J.G., Moncada-Herrera, J.A., 2008. A hybrid ARIMA and artificial neural networks model to forecast particulate matter in urban areas: the case of Temuco, Chile. Atmos. Environ. 42, 8331–8340.

Dockery, D., Pope, C., Xu, X.P., Spengler, J.D., Ware, J.H., Fay, M.E., Ferris, B.G., Speizer, F.E., 1993. An association between air-pollution and mortality in 6 United-states cities. N. Engl. J. Med. 329 (24), 1753–1759.

Doraiswamy, P., Hogrefe, C., Hao, W., Colle, B., Beauharnois, M., Demerjian, K., Ku, J.-Y., Sistla, G., 2009. Preliminary Experiences with the Multi-Model Air Quality Forecasting System for New York State, Paper presented at the 8th Annual Community Modeling and Analysis System (CMAS) Conference, Chapel Hill, NC.

Dutot, A.-L., Rynkiewicz, J., Steiner, F.E., Rude, J., 2007. A 24-h forecast of ozone peaks and exceedance levels using neural classifiers and weather predictions. Environ. Model. Software 22, 1261–1269. http://dx.doi.org/10.1016/j.envsoft.2006.08.002.

Eben, K., Juruŝ, P., Resler, J., Belda, M., Pelikán, E., Krüger, B.C., Keder, J., 2005. An ensemble Kalman filter for short-term forecasting of tropospheric ozone concentrations. Q. J. R. Meteorol. Soc. 131, 3313–3322.

Eder, B.K., Kang, D., Mathur, R., Yu, S., Schere, K., 2006. An operational evaluation of the Eta–CMAQ air quality forecast model. Atmos. Environ. 40, 4894–4905.

Eder, B., Kang, D., Rao, S.T., Mathur, R., Yu, S., Otte, T., Schere, K., Waylard, R., Jackson, S., Davidson, P., McQueen, J., Bridgers, G., 2010. Using national air quality forecast guidance to develop local air quality index forecasts. Bull. Amer. Meteor. Soc. 91, 313–326.

Elbern, H., Schmidt, H., 2001. Ozone episode analysis by four dimensional variational chemistry data assimilation. J. Geophys. Res. 106, 3569–3590.

Elbern, H., Friese, E., Strunk, A., 2010. EURAD-IM Products, Quality and Background Information. Report Prepared for MACC, Report D_R-ENS_1.3.2, March.

Elshout, S. v. d., Léger, K., 2007. Comparing Urban Air Quality across Borders – a Review of Existing Air Quality Indices and the Proposal of a Common Alternative. Final Report on the CITEAIR Project of the INTERREG IIIC programme, prepared by DCMR. Environmental Protection Agency Rijnmond, The Netherlands. June.

Ecological Society of America (ESA), 2004. Impacts of Atmospheric Pollution on Aquatic Ecosystems. In: Issues in Ecology, vol. 12. ISSN 1092-8987, The Ecological Society of America, Washington, DC, 20006, also Available at: http://www.esa.org/sbi/sbi_issues/, 26 pp.

European Union (EU), 2008. Directive 2008/50/EC of the European Parliament and of the Council of 21 May 2008 on ambient air quality and cleaner air for Europe. 11.6.2008, L. OJEU 152, 1–44.

Faraji, M., Kimura, Y., McDonald-Buller, E., Allen, D., 2008. Comparison of the carbon bond and SAPRC photochemical mechanisms under conditions relevant to southeast Texas. Atmos. Environ. 42, 5821–5836.

Fast, J.D., Gustafson Jr., W.I., Easter, R.C., Zaveri, R.A., Barnard, J.C., Chapman, E.G., Grell, G.A., Peckham, S.E., 2006. Evolution of ozone, particulates, and aerosol direct radiative forcing in the vicinity of Houston using a fully coupled meteorology-chemistry-aerosol model. J. Geophys. Res. 111, D21305. http://dx.doi.org/10.1029/2005JD006721.

Fast, J., et al., 2009. Evaluating simulated primary anthropogenic and biomass burning organic aerosols during MILAGRO: implications for assessing treatments of secondary organic aerosols. Atmos. Chem. Phys. 9, 6191–6215. http://dx.doi.org/10.5194/acp-9-6191-2009.

Flatøy, F., Hov, O., Schlager, H., 2000. Chemical forecasts used for measurement flight planning during POLINAT 2. Geophys. Res. Lett. 27, 951–954.

Flemming, J., Inness, A., Flentje, H., Huijnen, V., Moinat, P., Schultz, M.G., Stein, O., 2009. Coupling global chemistry transport models to ECMWF's integrated forecast system. Geosci. Model. Dev. 2, 253–265.

Folberth, G.A., Hauglustaine, D.A., Lathire, J., Rocheton, F., 2006. Interactive chemistry in the Laboratoire de Météorologie Dynamique general circulation model: model description and impact analysis of biogenic hydrocarbons on tropospheric chemistry. Atmos. Chem. Phys. 6, 2273–2319.

Forster, C., et al., 2004. Lagrangian transport model forecasts and a transport climatology for the Intercontinental Transport and Chemical Transformation 2002 (ITCT 2K2) measurement campaign. J. Geophys. Res. 109, D07S92. http://dx.doi.org/10.1029/2003JD003589.

Fountoukis, C., Nenes, A., 2005. Continued development of a cloud droplet formation parameterization for global climate models. J. Geophys. Res. 110, D11212. http://dx.doi.org/10.1029/2004JD005591.

Fraser, A., Davies, T., Lingard, J., 2010. Air Quality Forecasting with WRF and CMAQ, National Air Quality Forecasting Seminar, July 14. AEA, Harwell, UK.

Genc, D.D., Yesilyurt, C., Tuncel, G., 2010. Air pollution forecasting in Ankara, Turkey using air pollution index and its relation to assimilative capacity of the atmosphere. Environ. Monit. Assess. 166, 11–27. http://dx.doi.org/10.1007/s10661-009-0981-y.

Georgopoulos, et al., 2009. Air quality modeling needs for exposure assessment from the source-to-outcome perspective. Environ. Manage.. October Issue, 26-35.

Gilliam, R.C., Hogrefe, C., Rao, S.T., 2006. New methods for evaluating meteorological models used in air quality applications. Atmos. Environ. 40, 5073–5086.

Glahn, H.R., Lowry, D.A., 1972. The use of model output statistics (MOS) in objective weather forecasting. J. Appl. Meteorol. 11, 1203–1211.

Greenbaum, D.S., Bachmann, J.D., Krewski, D., Samet, J.M., White, R., Wyzga, R.E., 2001. Particulate air pollution standards and morbidity and mortality: case study. Am. J. Epidemiol. 154 (12). Supplement, S78–S90.

Grell, G., Dudhia, J., Stauffer, D., 1995. A Description of the Fifth-Generation Penn State/NCAR Mesoscale Model (MM5), NCAR Technical Note, NCAR/TN-398+STR.

Grell, G.A., Knoche, R., Peckham, S.E., McKeen, S.A., 2004. Online versus offline air quality modeling on cloud-resolving scales. Geophys. Res. Lett. 31, L16117. http://dx.doi.org/10.1029/2004GL020175.

Grell, G.A., Peckham, S.E., Schmitz, R., McKeen, S.A., . Frost, G., Skamarock, W.C., Eder, B., 2005. Fully coupled "online" chemistry within the WRF model. Atmos. Environ. 39, 6957–6975.

Gross, A., Stockwell, W.R., 2003. Comparison of the EMEP, RADM2, and RACM mechanisms. J. Atmos. Chem. 44, 151–170.

Gross, E., 1970. The National Air Pollution Potential Forecast Program. EESA Tech. Memo. WBTM NMC 47, ETAC TN 70-9. National Meteorological Center, Suitland, MD. November.

Guillas, S., Bao, J., Choi, Y., Wang, Y., 2008. Statistical correction and downscaling of chemical transport model ozone forecasts over Atlanta. Atmos. Environ. 42, 1338–1348. http://dx.doi.org/10.1016/j.atmosenv.2007.10.027.

Hadley, O.L., Ramanathan, V., Carmichael, G.R., Tang, Y., Corrigan, C.E., Roberts, G.C., Mauger, G.S., 2007. Trans-Pacific transport of black carbon and fine aerosols ($D < 2.5$ μm) into North America. J. Geophys. Res. 112, D05309. http://dx.doi.org/10.1029/2006JD007632.

Haldane, J., 1931. Atmospheric pollution and fogs. Br. Med. J., 366–367.

Han, Z.-W., Du, S.-Y., Lei, X.-E., Ju, L.-X., Wang, Q.-G., 2002. Numerical model system of urban air pollution prediction and its application. China Environ. Sci. 22 (3), 202–206 (in Chinese).

Hauglustaine, D.A., Hourdin, F., Jourdain, L., Filiberti, M.A., Walters, S., Lamarque, J.F., Holland, E.A., 2004. Interactive chemistry in the Laboratoire de Météorologie Dynamique general circulation model: description and background tropospheric chemistry evaluation. J. Geophys. Res. 109, D04314. http://dx.doi.org/10.1029/2003JD003957.

Hogrefe, C., Hao, W., Civerolo, K., Ku, J.-Y., Sistla, G., Gaza, R.S., Sedefian, L., Schere, K., Gilliland, A., Mathur, R., 2007. Daily simulation of ozone and fine particulates over New York State: findings and challenges. J. Appl. Meteorol. Climatol. 46 (7), 961–979. http://dx.doi.org/10.1175/JAM2520.1.

Hoi, K.I., Yuen, K.V., Mok, K.M., 2008. Kalman filter based prediction system for wintertime PM_{10} concentrations in Macau. Global NEST J. 10 (2), 140–150.

Honoré, C., Rouïl, L., Vautard, R., Beekmann, M., Bessagnet, B., Dufour, A., Elichegaray, C., Flaud, J.-M., Malherbe, L., Meleux, F., Menut, L., Martin, D., Peuch, A., Peuch, V.-H., Poisson, N., 2008. Predictability of European air quality: assessment of 3 years of operational forecasts and analysis by the PREV'AIR system. J. Geophys. Res. 113, D04301. http://dx.doi.org/10.1029/2007JD008761.

Jakobs, H.J., Tilmes, S., Heidegger, A., Nester, K., Smiatek, G., 2002. Short-term ozone forecasting with a network model system during summer 1999. J. Atmos. Chem. 42, 23–40.

Jayachandran, S., 2009. Air quality and early-life mortality: evidence from Indonesia's wildfires. J. Hum. Resour. 44 (4), 916–954.

Jiménez-Guerrero, P., Pérez, C., Jorba, O., Baldasano, J.M., 2008. Contribution of Saharan dust in an integrated air quality system and its on-line assessment. Geophys. Res. Lett. 35, L03814. http://dx.doi.org/10.1029/2007GL031580.

Jorquera, H., Perez, R., Cipriano, A., Espejo, A., Letelier, M.V., Acuna, G., 1998. Forecasting ozone daily maximum levels at Santiago, Chile. Atmos. Environ. 32, 3415–3424.

Kallos, G., Astitha, M., Katsafados, P., Spyrou, C., 2007. Long-range transport of anthropogenically and naturally produced particulate matter in the Mediterranean and North Atlantic: current state of knowledge. J. Appl. Meteorol. Climatol. 46, 1230–1251.

Kallos, G., Spyrou, C., Astitha, M., Mitsakou, C., Solomos, S., Kushta, J., Pytharoulis, I., Katsafados, P., Mavromatidis, E., Papantoniou, N., 2009. Ten-year operational

dust forecasting – Recent model development and future plans. IOP Conf. Ser.: Earth Environ. Sci. 7, 012012. http://dx.doi.org/10.1088/1755-1307/7/1/012012.
Kaminski, J.W., et al., 2008. GEM-AQ, an on-line global multiscale chemical weather modelling system: model description and evaluation of gas phase chemistry processes. Atmos. Chem. Phys. 8, 3255–3281.
Kang, D., Eder, B.K., Stein, A.F., Grell, G.A., Peckham, S.E., McHenry, J., 2005. The New England air quality forecasting pilot program: development of an evaluation protocol and performance benchmark. J. Air & Waste Manage. Assoc. 55, 1782–1796.
Kang, D., Mathur, R., Schere, K., Yu, S., Eder, B., 2007. New categorical metrics for air quality model evaluation. J. Appl. Meteorol. Climatol. 46, 549–555. http://dx.doi.org/10.1175/JAM2479.1.
Kang, D., Mathur, R., Rao, S.T., Yu, S., 2008. Bias adjustment techniques for improving ozone air quality forecasts. J. Geophys. Res. 113, D23308. http://dx.doi.org/10.1029/2008JD010151.
Kim, Y., Sartelet, K., Seigneur, C., 2009. Comparison of two gas-phase chemical kinetic Mechanisms of ozone formation over Europe. J. Atmos. Chem. 62, 89–119.
Kim, Y., Sartelet, K., Seigneur, C., 2011a. Formation of secondary aerosols: impact of the gas-phase chemical mechanism. Atmos. Chem. Phys. 11, 583–598. http://dx.doi.org/10.5194/acp-11-583-2011.
Kim, Y., Couvidat, F., Sartelet, K., Seigneur, C., 2011b. Comparison of different gas-phase mechanisms and aerosol modules for simulating particulate matter formation. J. Air Waste Manag. Assoc. 61, 1218–1226. http://dx.doi.org/10.1080/10473289.2011.603999.
Kondragunta, S., Lee, P., McQueen, J., Kittaka, C., Prados, A.I., Ciren, P., Laszlo, I., Pierce, R.B., Hoff, R., Szykman, J.J., 2008. Air quality forecast verification using satellite data. J. Appl. Meteor. Climatol. 47, 425–442.
Konovalov, I.B., Beekmann, M., Meleux, F., Dutot, A., Foret, G., 2009. Combining deterministic and statistical approaches for PM_{10} forecasting in Europe. Atmos. Environ. 43, 6425–6434. http://dx.doi.org/10.1016/j.atmosenv.2009.06.039.
Krupa, S.V., Grunhage, L., Jager, H.J., Nosal, M., Manning, W.J., Legge, A.H., Hanewald, K., 2006. Ambient ozone (O_3) and adverse crop response: a unified view of cause and effect. Environ. Pollut. 87, 119–126.
Kukkonen, J., et al., 2011. Operational, regional-scale, chemical weather forecasting models in Europe. Atmos. Chem. Phys. Discuss. 11, 5985–6162.
Kunzli, N., Kaiser, R., Medina, S., Studnicka, M., Filliger, P., Chanel, O., Herry, M., Horak, F., Puybonnieux-Texier, V., Quenel, P., Schneider, J., Seethaler, R., Vergnaud, J.C., Sommer, H., 2000. Public-health impact of outdoor and traffic-related air pollution: a European assessment. Lancet 356 (9232), 795–801.
Lawrence, M.G., et al., 2003. Global chemical weather forecasts for field campaign planning: predictions and observations of large-scale features during MINOS, CONTRACE, and INDOEX. Atmos. Chem. Phys. 3, 267–289.
Lee, A.M., Carver, G.D., Chipperfield, M.P., Pyle, J.A., 1997. Three dimensional chemical forecasting: a methodology. J. Geophys. Res. 102, 3905–3919.
Lee, P., Kang, D., McQueen, J., Tsisulko, M., Hart, M., DiMego, G., Seaman, N., Davidson, P., 2008. Impact of domain size on modeled ozone forecast for the Northeastern United states. J. Appl. Meteorol. Climatol. 47, 443–461. http://dx.doi.org/10.1175/2007JAMC1408.1.
Li, M., Hassan, R., 2010. Urban air pollution forecasting using artificial intelligence-based tools. In: Villanyi, Vanda (Ed.), Chpt. 9, Air Pollution. In Tech, ISBN 978-953-307-143-5, pp. 195–219.
Li, G., Zavala, M., Lei, W., Tsimpidi, A.P., Karydis, V.A., Pandis, S.N., Canagaratna, M.R., Molina, L.T., 2011. Simulations of organic aerosol concentrations in Mexico City using the WRF-CHEM model during the MCMA-2006/MILAGRO campaign. Atmos. Chem. Phys. 11, 3789–3809.
Luecken, D.J., Phillips, S., Sarwar, G., Jang, C., 2008. Effects of using the CB05 vs. SAPRC-99 vs. CB4 chemical mechanism on model predictions: ozone and gas-phase precursor concentrations. Atmos. Environ. 42, 5805–5820.
Mallet, V., Sportisse, B., 2006. Ensemble-based air quality forecasts: a multimodel approach applied to ozone. J. Geophys. Res. 111, D18302. http://dx.doi.org/10.1029/2005JD006675.
Mallet, V., Quélo, D., Sportisse, B., Ahmed de Biasi, M., Debry, É., Korsakissok, I., Wu, L., Roustan, Y., Sartelet, K., Tombette, M., Foudhil, H., 2007. Technical note: the air quality modeling system, Polyphemus. Atmos. Chem. Phys. 7 (20), 5479–5487.
Mallet, V., 2010. Ensemble forecast of analyses: coupling data assimilation and sequential aggregation. J. Geophys. Res. 115, D24303. http://dx.doi.org/10.1029/2010JD014259.
Manders, A.M.M., Schaap, M., Hoogerbrugge, R., 2009. Testing the capability of the chemistry transport model LOTOS-EUROS to forecast PM_{10} levels in the Netherlands. Atmos. Environ. 43, 4050–4059. http://dx.doi.org/10.1016/j.atmosenv.2009.05.006.
Mangold, A., De Backer, H., De Paepe, B., Dewitte, S., Chiapello, I., Derimian, Y., Kacenelenbogen, M., Léon, J.-F., Huneeus, N., Schulz, M., Ceburnis, D., O'Dowd, C., Flentje, H., Kinne, S., Benedetti, A., Morcrette, J.J., Boucher, O., 2011. Aerosol analysis and forecast in the European Centre for medium-range weather forecasts integrated forecast system: 3. Evaluation by means of case studies. J. Geophys. Res. 116, D03302.
Manins, P.C., Cope, M.E., Hess, G.D., Nelson, P.F., Puri, K., Wong, N., Young, M., 2002. The Australian air quality forecasting system: prognostic air quality forecasting in Australia. Clean Air and Environ. Quality 36 (2), 43–48.
Manins, P., October 1999. Air Quality Forecasting for Australia's Major Cities: 1st Progress Report; SB/1/407 25. CSIRO Atmospheric Research, Aspendale, Australia. http://www.dar.csiro.au/publications/Manins_1999a.pdf.
Matanoski, G.M., Tao, X., 2002. Case-cohort Study of Styrene Exposure and Ischemic Heart Disease. Research Report/Health Effects Institute, 108, pp. 1–29.
Mathur, R., Yu, S., Kang, D., Schere, K.L., 2008. Assessment of the wintertime performance of particulate matter forecasts with the Eta-Community Multi-scale Air Quality modeling system. J. Geophys. Res. 113, D02303. http://dx.doi.org/10.1029/2007JD008580.
McCollister, G., Wilson, K., 1975. Linear stochastic models for forecasting daily maxima and hourly concentrations of air pollutants. Atmos. Environ. 9, 417–423.
McHenry, J.N., Ryan, W.F., Seaman, N.L., Coats Jr., C.J., Pudykiewics, J., Arunachalam, S., Vukovich, J.M., 2004. A real-time Eulerian photochemical model forecast system: overview and initial ozone forecast performance in the Northeast U.S. corridor. Bull. Amer. Meteor. Soc. 85, 525–548.
McKeen, S., Wilczak, J., Grell, G., Djalova, I., Peckham, S., Hsie, E.-Y., Gong, W., Bouchet, V., Ménard, S., Moffet, R., McHenry, J., McQueen, J., Tang, Y., Carmichael, G.R., Pagowski, M., Chan, A., Dye, t., Frost, G., Lee, P., Mathur, R., 2005. Assessment of an ensemble of seven real-time ozone forecasts over eastern North America during the summer of 2004. J. Geophys. Res. 110, D21307. http://dx.doi.org/10.1029/2005JD005858.
McKeen, S., Chung, S.H., Wilczak, J., Grell, G., Djalalova, I., Peckham, S., Gong, W., Bouchet, V., Moffet, R., Tang, Y., Carmichael, G.R., Mathur, R., Yu, S., 2007. Evaluation of several $PM_{2.5}$ forecast models using data collected during the ICARTT/NEAQS 2004 field study. J. Geophys. Res. 112, D10S20. http://dx.doi.org/10.1029/2006JD007608.
McKeen, S., et al., 2009. An evaluation of real-time air quality forecasts and their urban emissions over eastern Texas during the summer of 2006 Second Texas Air Quality Study field study. J. Geophys. Res. 114, D00F11. http://dx.doi.org/10.1029/2008JD011697.
Menut, L., Bessagnet, B., 2010. Atmospheric composition forecasting in Europe. Ann. Geophys. 28, 61–74. www.ann-geophys.net/28/61/2010/.
Menut, L., Chiapello, I., Moulin, C., 2009. Previsibility of mineral dust concentrations: the CHIMERE-DUST forecast during the first AMMA experiment dry season. J. Geophys. Res. 114, D07202. http://dx.doi.org/10.1029/2008JD010523.
Merikanto, J., Napari, I., Vehkamäki, H., Anttila, T., Kulmala, M., 2007. New parameterization of sulfuric acid-ammonia-water ternary nucleation rates at tropospheric conditions. J. Geophys. Res. 112, D15207. http://dx.doi.org/10.1029/2006JD007977.
Michalakes, J., Chen, S., Dudhia, J., Hart, L., Klemp, J., Middlecoff, J., Skamarock, W., 2001. Development of a next-generation regional weather forecast model, Devel. In: Zwieflhofer, Walter, Kreitz, Norbert (Eds.), Teracomputing: Proceedings of the Ninth ECMWF Workshop on the Use of High Performance Computing in Meteorology. World Scientific, Singapore, pp. 269–276.
Millman, A., Tang, D.L., Perera, F.P., 2008. Air pollution threatens the health of children in China. Pediatrics 122, 620–628.
Misenis, C., Zhang, Y., 2010. An examination of WRF/Chem: physical parameterizations, nesting options, and grid resolutions. Atmos. Res. 97, 315–334.
Mitsakou, C., Kallos, G., Papantoniou, N., Spyrou, C., Solomos, S., Astitha, M., Housiadas, C., 2008. Saharan dust levels in Greece and received inhalation doses. Atmos. Chem. Phys. 8, 7181–7192.
Neary, L., Kaminski, J.W., Lupu, A., McConnell, J.C., 2007. Developments and Results from a Global Multiscale Air Quality Model (GEM-AQ). In: Air Pollution Modeling and Its Application XVII, vol. 5. http://dx.doi.org/10.1007/978-0-387-68854-1_44, pp. 403–410.
Niemeyer, L.E., 1960. Forecasting air pollution potential. Mon. Wee. Rev. 88 (3), 88–96.
Niu, T., Gong, S.L., Zhu, G.F., Liu, H.L., Hu, X.Q., Zhao, C.H., Wang, Y.Q., 2008. Data assimilation of dust aerosol observations for the CUACE/dust forecasting system. Atmos. Chem. Phys. 8, 3473–3482.
Ohara, T., Fujita, A., Kizu, T., Okamoto, S., 1997. Advanced air quality forecasting system for Chiba Prefecture, Proceedings of the 22nd NATO/CCMS International Technical Meeting on Air Pollution Modelling and its Application, Clermont-Ferrand, France, 2–6 June.
Otte, T.L., Pouliot, G., Pleim, J.E., Young, J.O., Schere, K.L., Wong, D.C., Lee, P.C.S., Tsidulko, M., McQueen, J.T., Davidson, P., Mathur, R., Chuang, H.-Y., DiMego, G., Seaman, N.L., 2005. NCEP Notes: linking the Eta model with the community multiscale air quality (CMAQ) modeling system to build a national air quality forecasting system. Weather Forecast. 20, 367–384.
Pagowski, M., Grell, G.A., 2006. Ensemble-based ozone forecasts: skill and economic value. J. Geophys. Res. 111, D23S30. http://dx.doi.org/10.1029/2006JD007124.
Pérez, P., Reyes, J., 2006. An integrated neural network model for PM_{10} forecasting. Atmos. Environ. 40, 2845–2851. http://dx.doi.org/10.1016/j.atmosenv.2006.01.010.
Peters, L.K., Berkowitz, C.M., Carmichael, G.R., Easter, R.C., Fairweather, G., Ghan, S.J., Hales, J.M., Ruby Leung, L., Pennell, W.R., Potra, F.A., Saylor, R.D., Tsang, T.T., 1995. The current state and future direction of Eulerian models in simulating the tropospheric chemistry and transport of trace species: a review. Atmos. Environ. 29, 189–222.
Phalen, R.F., Phalen, R.N., 2011. Introduction to Air Pollution Science. ISBN 10: 0763780448, Jones & Bartlett Learning.
Prybutok, V.R., Yi, J., Mitchell, D., 2000. Comparison of neural network models with ARIMA and regression models for prediction of Houston's daily maximum ozone concentrations. Eur. J. Oper. Res. 122, 31–40.
Pudykiewicz, J.A., Koziol, A.S., 2001. The application of Eulerian models for air quality prediction and the evaluation of emission control strategies in Canada. Int. J. Environ. Pollut. 16, 425–438.

Pudykiewicz, J.A., et al., 2003. Operational Air Quality Forecasting in Canada: Numerical Model Guidance for Ground-level Ozone and Particulate Matter, Preprints, Fifth Conf. on Atmospheric Chemistry: Gases, Aerosols, and Clouds, Long Beach, CA, Amer. Meteor. Soc., the 83rd Annual Meeting CD-ROM, 3.2.

Rasch, P.J., Mahowald, N.M., Eaton, B.E., 1997. Representations of transport, convection, and the hydrologic cycle in chemical transport models: Implications for the modeling of short-lived and soluble species. J. Geophys. Res. 102, 28127–28138.

Robertson, L., 2010. MATCH Products, Quality and Background Information, Report Prepared for MACC, Report D_R-ENS_1.5.2, March.

Roeckner, E., Brokopf, R., Esch, M., Giorgetta, M., Hagemann, S., Kornblueh, L., Manzini, E., Schlese, U., Schulzweida, U., 2006. Sensitivity of simulated climate to horizontal and vertical resolution in the ECHAM5 Atmosphere Model. J. Climate 19, 3771–3791.

Rouïl, L., Honoré, C., Vautard, R., Beekmann, M., Bssagnet, B., Malherbe, L., Meleux, F., Dufour, A., Elichegaray, C., Flaud, J.-M., Menut, L., Martin, D., Peuch, A., Peuch, V.-H., Poisson, N., 2009. Prev'air: an operational forecasting and mapping system for air quality in Europe. Bull. Amer. Meteor. Soc. 90, 73–83. http://dx.doi.org/10.1175/2008BAMS2390.1.

Rufeger, W., Mieth, P., Lux, T., 1997. Applying the DYMOS System in Conurbations, Proc. Modsim 97, 4. TAS, Australia, International Congress on Modelling and Simulation, Hobart, pp. 1797–1801.

Russell, A., Dennis, R., 2000. NARSTO critical review of photochemical models and modeling. Atmos. Environ. 34, 2283–2324.

Ryan, W.F., Petty, C.A., Luebehusen, E.D., 2000. Air quality forecasts in the mid-Atlantic region: current practice and benchmark skill. Weather Forecast. 15, 46–60.

Ryan, W.F., 1995. Forecasting ozone episodes in the Baltimore metropolitan area. Atmos. Environ. 29 (17), 2387–2398.

San José, R., Pérez, J.L., González, R.M., 2006. CFD and Mesoscale Air Quality Application in Urban Environment: MADRID Case Study, Proceedings of the 4th WSEAS International Conference on Environment, Ecosystems, and Development (EED '06), Venice, Italy, November 20–22, 2006

San José, R., Pérez, J.L., Morant, J.L., González Barras, R.M., 2009. The use of Modern third-generation air quality models (MM5-EMIMO-CMAQ) for real-time operational air quality impact assessment of industrial plants. Water Air Soil Pollu.: Focus 9 (1–2), 27–37. http://dx.doi.org/10.1007/s11267-008-9196-4.

Sartelet, K.N., Debry, E., Fahey, K., Roustan, Y., Tombette, M., Sportisse, B., 2007. Simulation of aerosols and gas-phase species over Europe with the Polyphemus system: Part I-Model-to-data comparison for 2001. Atmos. Environ. 41, 6116–6131. http://dx.doi.org/10.1016/j.atmosenv.2007.04.024.

Schaap, M., Timmermans, R.M.A., Sauter, F.J., Roemer, M., Velders, G.J.M., Boersen, G.A.C., Beck, J.P., Builtjes, P.J.H., 2008. The LOTOS-EUROS model: description, validation and latest developments. Int. J. Environ. Pollut. 32 (2), 270–289.

Schere, K., Bouchet, V., Grell, G., McHenry, J., McKeen, S., 2006. The Emergence of Numerical Air Quality Forecasting Models and Their Applications, presentation at The AMS Forum on Managing Our Physical and Natural Resources, February 2, Atlanta, GA.

Schwartz, J., 1991. Particulate air pollution and daily mortality in Detroit. Environ. Res. 56, 204–213.

Seigneur, C., et al., 2000. Guidance for the performance evaluation of three-dimensional air quality modeling systems for particulate matter and visibility. J. Air Waste Manage. Assoc. 50, 588–599.

Seigneur, C., 1994. The status of mesoscale air quality models. In: Solomon, P. (Ed.), Planning and Managing Air Quality Modeling and Measurement Studies: a Perspective Through SJVAQS/AUSPEX. Lewis Publishers, Boca Raton, Florida, U.S.A, pp. 403–433 (Chapter 3-2).

Seigneur, C., 2001. Current status of air quality modeling for particulate matter. J. Air Waste Manage. Assoc. 51, 1508–1821.

Seinfeld, J.H., Pandis, S.N., 2006. Atmospheric Chemistry and Physics: From Air Pollution to Climate Change. John Wiley & Sons, Inc., ISBN 978-0-471-72018-8.

Shad, R., Mesgari, M.S., Abkar, A., Shad, A., 2009. Predicting air pollution using fuzzy genetic linear membership kriging in GIS. Comput. Environ. Urban. 33, 472–481.

Shrivastava, M., Fast, J., Easter, R., Gustafson Jr., W.I., Zaveri, R.A., Jimenez, J.L., Saide, P., Hodzic, A., 2010. Modeling organic aerosols in a megacity: comparison of simple and complex representations of the volatility basis set approach. Atmos. Chem. Phys. Discuss. 10, 30205–30277.

Sihto, S., Kulmala, M., Kerminen, V., Dal Maso, M., Petäjä, T., Riipinen, I., Korhonen, H., Arnold, F., Janson, R., Boy, M., 2006. Atmospheric sulphuric acid and aerosol formation: Implications from atmospheric measurements for nucleation and early growth mechanisms. Atmos. Chem. Phys. 6, 4079–4091. http://dx.doi.org/10.5194/acp-6-4079-2006.

Sofiev, M., Vira, J., 2010. SILAM Products, Quality and Background Information. Report Prepared for MACC, Report D_R-ENS_1.9.2, March.

Sofiev, M., Siljamo, P., Ranta, H., Rantio-Lehtimäki, A., 2006. Towards numerical forecasting of long-range air transport of birch pollen: theoretical considerations and a feasibility study. Int. J. Biometeorol. 50, 392–402.

Spyrou, C., Mitsakou, C., Kallos, G., Louka, P., Vlastou, G., 2010. An improved limited area model for describing the dust cycle in the atmosphere. J. Geophys. Res. 115, D17211. http://dx.doi.org/10.1029/2009JD013682.

Stadlober, E., Hörmann, S., Pfeiler, B., 2008. Quality and performance of a PM_{10} daily forecasting model. Atmos. Environ. 42, 1098–1109. http://dx.doi.org/10.1016/j.atmosenv.2007.10.073.

Stockwell, W.R., et al., 2002. The scientific basis of NOAA's air quality forecast program. Environ. Manage.. December, 20–27.

Stohl, A., Forster, C., Frank, A., Seibert, P., Wotawa, G., 2005. Technical note: the Lagrangian particle dispersion model FLEXPART version 6.2. Atmos. Chem. Phys. 5, 2461–2474.

Takigawa, M., Niwano, M., Akimoto, H., Takahashi, M., 2007. Development of a one-way nested global-regional air quality forecasting model. SOLA 3, 81–84. http://dx.doi.org/10.2151/sola.2007–021.

Talbot, D., 2007. Development of a New Canadian Operational Air Quality Forecast Model GEM-MACH, paper presented at the International Technical Meeting on Air Pollution Modelling and its Application, Aveiro-Portugal, 24–28 September.

Tie, X., Geng, F.H., Peng, L., Gao, W., Zhao, C.S., 2009. Measurement and modeling of O_3 variability in Shanghai, China; application of the WRF-Chem model. Atmos. Environ. 43, 4289–4302.

Tilmes, S., et al., 2002. Comparison of five Eulerian air pollution forecasting systems for the summer of 1999 using the German ozone monitoring data. J. Atmos. Chem. 42, 91–121.

U.S. (EPA), 1996. Air Quality Criteria for Particulate Matter. Research Triangle Park, N.C.: Office of Research and Development, Office of Health and Environmental Assessment. EPA report no. EPA/600/P-95/001aF.

U.S. EPA, 1999. Guideline for Developing an Ozone Forecasting Program. U.S. Environmental Protection Agency Rep, EPA-454/R-99–009, 88 pp. Available from: Office of Air Quality Planning and Standards, EPA, Research Triangle Park, NC 27711.

U.S. EPA, 2000. Air Quality Index, a Guide to Air Quality and Your Health. EPA-454/R-00-005. U.S. Environmental Protection Agency, Office of Air and Radiation, Washington, DC. http://www.epa.gov/airnow/aqibroch.

U.S. EPA, 2001. Guidance for Demonstrating Attainment of Air Quality Goals for $PM_{2.5}$ and Regional Haze, Draft 2.1, January 2, 2001. The U.S. Environmental Protection Agency, Office of Air and Radiation/Office of Air Quality Planning and Standards, Research Triangle Park, NC 27711.

U.S. EPA, 2003. Guideline for Developing an Air Quality (Ozone and $PM_{2.5}$) Forecasting Program. U.S. Environmental Protection Agency Rep, EPA-456/R-03-002, 126 pp. Available from: Office of Air Quality Planning and Standards, EPA, Research Triangle Park, NC 27711; Also Available Online at: http://www.epa.gov/airnow/aq_forecasting_guidance-1016.pdf.

U.S. EPA, 2009. Technical Assistance Document for Reporting of Daily Air Quality—Air Quality Index (AQI). EPA-454/B-09-001. U.S. Environmental Protection Agency, Office of Air Quality Planning and Standards, Research Triangle Park, NC.

Uno, I., et al., 2003. Regional chemical weather forecasting system CFORS: model descriptions and analysis of surface observations at Japanese island stations during the ACE-Asia experiment. J. Geophys. Res. 108, 8668. http://dx.doi.org/10.1029/2002JD002845.

Valdebenito, B., Benedictow, Á.M., A.C., 2010. EMEP Products, Quality and Background Information, Report Prepared for MACC, Report D_R-ENS_1.2.2, March.

van der Wal, J.T., Jansen, L.H.J.M., 2000. Analysis of spatial and temporal variations of PM_{10} concentrations in the Netherlands using Kalman filtering. Atmos. Environ. 34, 3675–3687.

Vaughan, J., et al., 2004. A numerical daily air quality forecast system for the Pacific Northwest. Bull. Amer. Meteor. Soc. 85, 549–561.

Vautard, R., Blond, N., Schmidt, H., Derognat, C., Beekmann, M., 2001a. Multi-model ensemble ozone forecasts over Europe: analysis of uncertainty. In: Brandt, J. (Ed.), Mesoscale Transport of Air Pollution. OA15. EGS XXXVI General Assembly. Nice. European Geophysical Society, Katlenburg-Lindau, Germany, France. 26 March.

Vautard, R., Beekmann, M., Roux, J., Gombert, D., 2001b. Validation of a deterministic forecasting system for the ozone concentrations over the Paris area. Atmos. Environ. 35, 2449–2461.

Wang, Z.-F., Wu, Q.-Z., Gbaguidi, A., Yan, P.-Z., Zhang, W., Wang, W., Tang, X., 2009. Ensemble air quality multi-model forecast system for Beijing (EMS-Beijing): model description and preliminary application. J. of NUIST: Natural Science Edition 1 (1), 19–26 (in Chinese).

Wang, X., Mallet, V., Berroir, J.-P., Herlin, I., 2011. Assimilation of OMI NO2 retrievals into a regional chemistry-transport model for improving air quality forecasts over Europe. Atmos. Environ. 45, 485–492.

Wayland, R.A., White, J.E., Dickerson, P.G., Dye, T.S., 28-36, December 2002. Communicating real-time and forecasted air quality to the public. Environ. Manage.

Wilby, R.L., Wigley, T.M.L., 1997. Downscaling general circulation model output: a review of methods and limitations. Prog. Phys. Geog. 21, 530–548.

Wilczak, J., McKeen, S., Djalalova, I., Grell, G., Peckam, S., Gong, W., Bouchet, V., Moffet, R., McHenry, J., Mc-Queen, J., Lee, P., Tang, Y., Carmichael, G.R., 2006. Bias-corrected ensemble and probabilistic forecasts of surface ozone over eastern North America during the summer of 2004. J. Geophys. Res. 111, D23S28. http://dx.doi.org/10.1029/2006JD007598.

Willmott, C.J., 1981. On the validation of models. Phys. Geogr. 2, 184–194.

Wilson, L.J., Valée, M., 2003. The Canadian Updateable Model Output Statistics (UMOS) system: validation against perfect prog. Weather Forecast. 18, 288–302.

Wolff, G.T., Lioy, P.J., 1978. An empirical model for forecasting maximum daily ozone levels in the northeastern United States. J. Air Pollut. Control Assoc. 28, 1034–1038.

World Health Organization (WHO), 2004. Health Aspects of Air Pollution, Results from the WHO Project "Systematic Review of Health Aspects of Air Pollution in Europe, " June, E83080. World Health Organization, Regional Office for Europe Scherfigsvej 8, DK-2100 Copenhagen Ø, Denmark.

World Health Organization (WHO), 2010. WHO Guidelines for Indoor Air Quality: Selected Pollutants. World Health Organization, egional Office for Europe Scherfigsvej 8, DK-2100 Copenhagen Ø, Denmark, ISBN 9789289002134.
Wu, L., Mallet, V., Bocquet, M., Sportisse, B., 2008. A comparison study of data assimilation algorithms for ozone forecasts. J. Geophys. Res. 113, D20310. http://dx.doi.org/10.1029/2008JD009991.
Yu, S.C., Eder, B., Dennis, R., Chu, S.-H., Schwartz, S., 2006. New unbiased symmetric metrics for evaluation of air quality models. Atmos. Sci. Lett. 7, 26–34.
Yu, S.C., Mathur, R., Kang, D., Schere, K., Pleim, J., Otte, T.L., 2007. A detailed evaluation of the Eta-CMAQ forecast model performance for O_3, its related precursors, and meteorological parameters during the 2004 ICARTT study. J. Geophys. Res. 112, D12S14. http://dx.doi.org/10.1029/2006JD007715.
Yu, S., Mathur, R., Schere, K., Kang, D., Pleim, J., Young, J., Tong, D., Pouliot, G., McKeen, S.A., Rao, S.T., 2008. Evaluation of real-time $PM_{2.5}$ forecasts and process analysis for $PM_{2.5}$ formation over the eastern United States using the Eta-CMAQ forecast model during the 2004 ICARTT study. J. Geophys. Res. 113, D06204. http://dx.doi.org/10.1029/2007JD009226.
Yu, F., 2010. Ion-mediated nucleation in the atmosphere: key controlling parameters, implications, and look-up table. J. Geophys. Res. 115, D03206. http://dx.doi.org/10.1029/2009JD012630.
Zhang, Y., Liu, P., Pun, B., Seigneur, C., 2006a. A comprehensive performance evaluation of MM5-CMAQ for the summer 1999 southern oxidants study episode, part-I. Evaluation protocols, databases and meteorological predictions. Atmos. Environ. 40, 4825–4838.
Zhang, Y., Liu, P., Queen, A., Misenis, C., Pun, B., Seigneur, C., Wu, S.-Y., 2006b. A comprehensive performance evaluation of MM5-CMAQ for the summer 1999 southern oxidants study episode, Part-II. Gas and aerosol predictions. Atmos. Environ. 40, 4839–4855.
Zhang, K., Wan, H., Wang, B., Zhang, M., Feichter, J., Liu, X., 2010. Tropospheric aerosol size distributions simulated by three online global aerosol models using the M7 microphysics module. Atmos. Chem. Phys. 10, 6409–6434. http://dx.doi.org/10.5194/acp-10-6409-2010.
Zhang, Y., Pan., Y., Wang, K., Fast, J.D., Grell, G.A., 2010a. WRF/Chem-MADRID: incorporation of an aerosol module into WRF/Chem and its initial application to the TexAQS2000 episode. J. Geophys. Res. 115, D18202. http://dx.doi.org/10.1029/2009JD013443.
Zhang, Y., Liu, P., Liu, X.-H., Pun, B., Seigneur, C., Jacobson, M.Z., Wang, W.-X., 2010b. Fine scale modeling of wintertime aerosol mass, number, and size distributions in Central California. J. Geophys. Res. 115, D15207. http://dx.doi.org/10.1029/2009JD012950.
Zhang, Y., Wen, X.-Y., Jang, C.J., 2010c. Simulating climate-chemistry-aerosol-cloud-radiation feedbacks in continental U.S. using online-coupled WRF/Chem. Atmos. Environ. 44 (29), 3568–3582.
Zhang, Y., Chen, Y.-S., Zhu, S., Wu, S.-Y., Sartelet, K., Tran, P., Seigneur, C., 2011. Application of WRF/Chem-MADRID in Europe: Model Evaluation and Aerosol-Meteorology Interactions, Presentation at the EGU General Assembly 2011. Vienna, Austria, 3–8 April.
Zhang, Y., Karamchandani, P., Glotfelty, T., Streets, D.G., Grell, G., Nenes, A., Yu, F.-Q., Bennartz, R., 2012. Development and Initial Application of the Global-Through-Urban Weather Research and Forecasting Model with Chemistry (GU-WRF/Chem). J. Geophys. Res., in review.
Zhang, Y., Chen, Y.-C., Sarwar, G., Schere, K., 2012. Impact of gas-phase mechanisms on WRF/Chem predictions: mechanism implementation and comparative evaluation. J. Geophys. Res. 117, D1. http://dx.doi.org/10.1029/2011JD015775.
Zhang, Y., 2008. Online coupled meteorology and chemistry models: history, current status, and outlook. Atmos. Chem. Phys. 8, 2895–2932.
Zolghadri, A., Cazaurang, F., 2006. Adaptive nonlinear state-space modelling for the prediction of daily mean PM10 concentrations. Environ Model. Software 21, 885–894. http://dx.doi.org/10.1016/j.envsoft.2005.04.008.